WT-1679 (EX)
EXTRACTED VERSION

12

OPERATiON HARDTACK

Projects 2.4a/2.11/2.12a
Neutron Flux From Very-Low-Yield Bursts

April-October 1958

Headquarters Field Command
Defense Atomic Support Agency
Sandia Base, Albuquerque, New Mexico

August 31, 1960

NOTICE

This is an extract of WT-1679, which remains classified SECRET/RESTRICTED DATA as of this date.

Extract version prepared for:

Director
DEFENSE NUCLEAR AGENCY
Washington, D.C. 20305

1 OCTOBER 1983

SECURITY CLASSIFICATION OF THIS PAGE (When Data Entered)

REPORT DOCUMENTATION PAGE

READ INSTRUCTIONS BEFORE COMPLETING FORM

1. REPORT NUMBER: WT-1679 (EX)
2. GOVT ACCESSION NO.: AD-A995 191
3. RECIPIENT'S CATALOG NUMBER:
4. TITLE (and Subtitle): Operation HARDTACK - Projects 2.4a/2.11/2.12a Neutron Flux From Very-Low-Yield Bursts
5. TYPE OF REPORT & PERIOD COVERED:
6. PERFORMING ORG. REPORT NUMBER: WT-1679 (EX)
7. AUTHOR(s): D. L. Rigotti, J. L. Tarbox, T. R. Adams, J. W. Kinch, N. Klein, J. H. McNeilly, P. A. Pankow
8. CONTRACT OR GRANT NUMBER(s):
9. PERFORMING ORGANIZATION NAME AND ADDRESS: U.S. Army Chemical Warfare Laboratories, Army Chemical Center, Maryland
10. PROGRAM ELEMENT, PROJECT, TASK AREA & WORK UNIT NUMBERS:
11. CONTROLLING OFFICE NAME AND ADDRESS: Headquarters Field Command, Defense Atomic Support Agency, Sandia Base, Albuquerque, New Mexico
12. REPORT DATE: August 31, 1960
13. NUMBER OF PAGES:
14. MONITORING AGENCY NAME & ADDRESS (if different from Controlling Office):
15. SECURITY CLASS. (of this report): UNCLASSIFIED
15a. DECLASSIFICATION/DOWNGRADING SCHEDULE:
16. DISTRIBUTION STATEMENT (of this Report): Approved for public release; unlimited distribution.
17. DISTRIBUTION STATEMENT (of the abstract entered in Block 20, if different from Report):
18. SUPPLEMENTARY NOTES: This report has had the classified information removed and has been republished in unclassified form for public release. This work was performed by Kaman Tempo under contract DNA001-79-C-0455 with the close cooperation of the Classification Management Division of the Defense Nuclear Agency.
19. KEY WORDS (Continue on reverse side if necessary and identify by block number): Operation HARDTACK; Neutron Flux
20. ABSTRACT (Continue on reverse side if necessary and identify by block number): The objectives of these projects were to: (1) measure neutron flux and dose versus ground range for very-low-yield (fractional-kiltoton) nuclear devices; (2) measure neutron, thermal, and gamma radiation up to an altitude of 1,500 feet; (3) provide dose measurements in support of a biomedical project (Project 4.2); and (4) determine neutron flux and spectrum for induced-activity studies (Project 2.12c).

DD FORM 1 JAN 73 1473 EDITION OF 1 NOV 65 IS OBSOLETE

SECURITY CLASSIFICATION OF THIS PAGE (When Data Entered)

FOREWORD

This report has had classified material removed in order to make the information available on an unclassified, open publication basis, to any interested parties. This effort to declassify this report has been accomplished specifically to support the Department of Defense Nuclear Test Personnel Review (NTPR) Program. The objective is to facilitate studies of the low levels of radiation received by some individuals during the atmospheric nuclear test program by making as much information as possible available to all interested parties.

The material which has been deleted is all currently classified as Restricted Data or Formerly Restricted Data under the provision of the Atomic Energy Act of 1954, (as amended) or is National Security Information.

This report has been reproduced directly from available copies of the original material. The locations from which material has been deleted is generally obvious by the spacings and "holes" in the text. Thus the context of the material deleted is identified to assist the reader in the determination of whether the deleted information is germane to his study.

It is the belief of the individuals who have participated in preparing this report by deleting the classified material and of the Defense Nuclear Agency that the report accurately portrays the contents of the original and that the deleted material is of little or no significance to studies into the amounts or types of radiation received by any individuals during the atmospheric nuclear test program.

FOREWORD

This report presents the final results of three of the projects participating in the military-effect programs of Operation Hardtack. Overall information about these and the other military-effect projects can be obtained from ITR-1660, the "Summary Report of the Commander, Task Unit 3." This technical summary includes: (1) tables listing each detonation with its yield, type, environment, meteorological conditions, etc.; (2) maps showing shot locations; (3) discussions of results by programs; (4) summaries of objectives, procedures, results, etc., for all projects; and (5) a listing of project reports for the military-effect programs.

ABSTRACT

The objectives of these projects were to: (1) measure neutron flux and dose versus ground range for very-low-yield (fractional-kiloton) nuclear devices; (2) measure neutron, thermal, and gamma radiation up to an altitude of 1,500 feet; (3) provide dose measurements in support of a biomedical project (Project 4.2); and (4) determine neutron flux and spectrum for induced-activity studies (Project 2.12c).

The threshold-detector technique was used to measure neutron flux; gold, plutonium, neptunium, uranium, and sulfur were the detecting materials. National Bureau of Standards (NBS) film badges were used to measure total gamma dose. Chemical Warfare Laboratories thermistor calorimeters were employed for thermal measurements. For Shot Quince, an Aerocap balloon was used to support the instrument line almost directly above ground zero, and thirteen stations were instrumented for slant ranges from 40 to 500 yards. For Shot Fig, an Aerocap balloon was tethered on a single cable 120 yards laterally from ground zero. Because of bad weather conditions that reduced the lift of the balloon, the thermal detectors were eliminated, and neutron and gamma detectors were installed at slant ranges of 121 to 410 yards. For Shots Hamilton and Humboldt, in addition to the standard-foil system, a chemical-dosimeter system was employed to measure neutron and gamma dose simultaneously. The instrumentation consisted of two glass vials of saturated aqueous solution of trichloroethylene that differed in their dissolved oxygen content.

Within the range of neutron measurements, there was no variation of the neutron-energy spectrum above the plutonium threshold (10 kev) with increasing distance.

Personnel stationed more than 1,000 yards from ground zero would have received negligible neutron dose.

Gamma doses of 4,200 r and 350 r, respectively, were measured at the same altitudes. Since the thermal detectors were eliminated from the balloon stations, no thermal results were obtained.

Results at the balloon stations were higher by average factors of and 3.3 for gamma radiation than those observed at equivalent distances along the ground.

The balloon technique for instrument location is effective for free-air measurements.

During Shots Hamilton and Humboldt, neutron fluxes were measured by the threshold-detector technique in support of the biomedical Project 4.2. Also, neutron flux and spectrum were measured for Shot Hamilton in support of Project 2.12c. No variation of the neutron-energy spectrum above 10 kev with increasing distance from the point of detonation for either shot was observed beyond 150 yards.

Best estimates indicate that a man stationed without shielding at 600 yards from ground zero would have received from Shot Hamilton and from Shot Humboldt.

The chemical-dosimetry technique resulted in no useful data.

No results were obtained from Shot Quince because of the absence of nuclear yield.

PREFACE

The authors express their appreciation to Payne Harris, Don Ott, and Joseph Sayeg, of the Los Alamos Scientific Laboratory, who assisted in calibration of neutron detectors and chemical dosimeters. The aid of G. S. Hurst and Paul Reinhart of the Oak Ridge National Laboratory during cross-calibration at their laboratory, is also greatly appreciated.

The authors express their deep appreciation for the support, encouragement, and understanding accorded them personally by CAPT Mendenhall, USN, Commander, Task Unit 3 (Shot Fig), and by his staff during the execution of the field phase of Project 2.11. Particular thanks are extended to the Task Unit 3 Operations Group of Lt Col Dickenson, Lt Col Isengard, Capts Thomas and Sheehan, and CWO Osborne who, with the General Mills' balloon group, were responsible to a major extent for the success of our participation in this shot.

CONTENTS

FIGURES

Chapter 1
INTRODUCTION

1.1 OBJECTIVES

The objectives of these projects were to: (1) measure neutron flux and dose versus ground range for very-low-yield (fractional-kiloton) nuclear devices; (2) measure neutron, thermal, and gamma radiation up to an altitude of 1,500 feet; (3) provide dose measurements in support of a biomedical project (Project 4.2); and (4) determine neutron flux and spectrum for induced-activity studies (Project 2.12c).

1.2 BACKGROUND

Neutron flux has been measured at almost all nuclear-weapon tests since Operation Sandstone (References 1 through 7). It is documented for two reasons: First, the documentation is needed by weapon-development laboratories for diagnosing and evaluating the performance of the nuclear device. Second, it is used by Department of Defense agencies as effects information. The documentation of the number and energy of the neutrons versus ground range for a specific device is used in evaluating the effects of the neutrons on the environment external to the device. The establishment of the number and energy of the neutrons is commonly referred to as neutron-flux measurements.

1.2.1 Past Operations. Neutron flux has been measured for devices with a wide range of yields; however, the only results obtained in the 0-to-100-ton range of yields were those from Shot Franklin of Operation Plumbbob (Reference 6). Particular interest has been attached to this yield range with the advent of the proposed battle-group delivery system for which devices of this type would be candidate weapons.

Original Department of the Army proposals for the testing of a device in this yield range as part of Operation Trumpet, scheduled for the spring of 1959, visualized first two, then later, three shots at three different burst heights: surface, one-fireball radius, and greater than one-fireball radius. This testing was intended to clearly delineate the fallout problem, the hazard of induced activity in the soil, blast, and the effects of thermal and initial nuclear radiation. It was planned that all the necessary measurements would be made by ground stations in the manner employed during previous operations.

Because of an impending nuclear-test ban, which finally became effective 31 October 1958, many changes in weapon-test plans were made. One of these changes consisted of the inclusion of all the original proposals for measuring effects during a single surface detonation. However, the question arose as to the ability to satisfactorily document the thermal, initial gamma, and neutron radiation because of the line-of-sight geometry requirement for these measurements. Use of a balloon, with an instrument line suspended almost directly above the device was suggested as the best method of obtaining the desired geometry.

Balloons had been successfully used during Operation Plumbbob to support nuclear devices and (Reference 8) to support instrumentation. Accordingly, plans were made to use balloons to obtain the required line-of-sight geometry for the above-mentioned measurements.

Additionally, since measurements made on a low-yield, device indicated that the casualty-producing area of neutrons may exceed that of the blast and other radiation effects, a study of the biomedical effects of neutrons was deemed of utmost importance. This study was to be accomplished by the exposure of large animals (pigs) in various environments at several distances from a low-yield nuclear detonation at the Nevada Test Site (NTS).

1.2.2 Methods. The threshold-detector technique presently offers the most-reliable method of measuring neutrons emitted from nuclear detonations. This method utilizes chemical elements that are activated through nuclear transformations involving neutron capture or fission. The radioactive products of these transformations are directly proportional to the neutron flux to which the detectors were exposed and can be correlated directly with it. Table 1.1 lists the elements, threshold energy, and type of activation usually employed in the threshold-detector technique.

Since Operation Teapot, several laboratories have used threshold detectors to measure neutron flux (References 4 through 7), and excellent results have been obtained. The measurements may be used to calculate the neutron dose by the use of a single-collision theory of dose contri-

TABLE 1.1 NEUTRON DETECTORS

Detector	Threshold Energy, E_i	Reaction
Gold	Thermal energies up to 0.3 ev	$Au^{197}(n,\gamma)Au^{198}$
Pu^{239}	10 kev (w/B^{10} shield)	Fission
Np^{237}	0.63 Mev	Fission
U^{238}	1.5 Mev	Fission
Sulfur	3.0 Mev	$S^{32}(n,p)P^{32}$
Zirconium	12.3 Mev	$Zr^{90}(n,2n)Zr^{89}$

bution per neutron (References 9 and 10). Neutron dose calculated in this manner agrees well with measurements made by the previously developed Hurst proportional counter.

A second method of measuring dose from neutron radiation is by the use of chemical reactions in an aqueous solution. This method is generally called chemical dosimetry. Chemical-dosimetry systems have been employed in laboratory work with gamma radiation for many years with excellent results (References 11, 12, and 13). However, most of these systems require carefully controlled exposures, as well as complex equipment and techniques.

In theory, the aqueous system has a response to radiation similar to that of tissue. This is assumed to be true, because tissue is primarily water and will, therefore, have energy-transfer properties similar to those observed in aqueous solution. The Chemical Warfare Laboratories (CWL) are developing an aqueous system that is to be capable of measuring the combined gamma-neutron dose from exposure to radiation from nuclear detonations. This system has been shown to record gamma dose, but the response of the system to a combined gamma-neutron dose has been determined for only a narrow range of neutron energies.

The CWL chemical-dosimetry system employs a saturated aqueous solution of trichloroethylene (TCE) contained in two round glass vials. It responds to radiation by producing acids and polymers. Measurements of radiation are dependent upon determination of the total acid produced. In the high-purity and unbuffered solutions, the change in pH is a measure of the amount of radiation to which the system has been exposed. It has been found that the gamma response may be varied, with neutron response being unaffected, by the changing of the oxygen content of the atmosphere in which the tubes are filled and sealed. The system is inherently insensitive to alpha and beta radiation, because of its glass container, and is heat and light stable.

The original plans, as of January 1958, did not call for any chemical-dosimetry measurements in the field prior to Operation Trumpet. It was hoped that by the advent of Operation Trumpet, the laboratory studies on the neutron response of the system would have been completed. As the forecasts of an impending nuclear-test suspension became more and more persistent, the need was felt for some indication of the response under field conditions. This led

to the use of the system during Operation Hardtack. Now that the test participation has been completed, plans are underway for extensive evaluation of the system, utilizing the neutron-producing equipment available at the Los Alamos Scientific Laboratory (LASL) and the Brookhaven National Laboratories (BNL).

1.3 THEORY

1.3.1 Neutron Production. The fission process is well known and needs no further discussion here. It suffices to say that a certain fraction of the total number of neutrons produced is necessary to maintain the fission process. The neutrons that escape must pass through the material of the device and, in doing so, may be absorbed or scattered by the material. In general, the scattering process results in a degradation of the energy of the neutrons and a change of their angular distribution, while that of absorption completely removes the neutrons from the system. As the neutrons pass into the air, the absorption and scattering processes continue.

Thus, the number of neutrons that reach a given volume in space outside the device will consist of those neutrons that escape the scattering and absorption processes, plus an additional number of neutrons that have been scattered. Any quantitative estimation of the number and energy of neutrons reaching a finite volume of space outside the device must take into consideration the reduction of the number of neutrons due to the spherical geometry of the problem. A mathematical formulation of this problem has been given by the Boltzman transport equation (Reference 5).

The balloon technique, effectively allowing the detectors to "look down" at the device, maximizes line-of-sight geometry enabling free-air measurements. When compared with air-surface interface measurements, these free-air measurements should provide a good indication of neutron albedo for a particular area.

1.3.2 Threshold Detectors. The reactions of interest have been previously listed in Table 1.1. From this table, it is seen that both gold and sulfur are converted into radioactive isotopes by neutron capture, and radioactive fission products are produced by the fission processes occurring when plutonium, neptunium, or uranium are bombarded with neutrons.

A more-complete description of these reactions is given in Reference 14, and a description of the detectors is presented in Section 2.2.1.

1.3.3 Chemical Dosimetry. The CWL chemical-dosimetry system utilized an aqueous solution of TCE. This system responds differently to gamma and neutron radiations, which will be discussed separately.

The transfer of gamma-ray energy into water is a moderately complex process. The mechanism wherein the absorption of energy by aqueous TCE results in the production of acids is not known with certainty, and there are probably several plausible explanations for this process. The mechanism described herein adequately explains all of the phenomena observed to date and successfully predicts the observed reaction products.

When gamma radiation transfers its energy to water or dilute aqueous solutions, decomposition occurs as shown in Reaction 1.1:

$$H_2O \longrightarrow H^{\cdot} + OH^{\cdot} \qquad (1.1)$$

These radicals can then react with each other or with the solutes present as is shown by the following reactions:

$$H^{\cdot} + H^{\cdot} \longrightarrow H_2 \qquad (1.2)$$

$$OH^{\cdot} + OH^{\cdot} \longrightarrow H_2O_2 \qquad (1.3)$$

$$H^{\cdot} + O_2 \longrightarrow HO_2^{\cdot} \qquad (1.4)$$

$$H^{\cdot} + \begin{matrix} H & & Cl \\ & \diagdown\ \diagup & \\ & C=C & \\ & \diagup\ \diagdown & \\ Cl & & Cl \end{matrix} \longrightarrow \begin{matrix} Cl & Cl \\ | & | \\ H-C-C^{\cdot} \\ | & | \\ H & Cl \text{ (etc.)} \end{matrix} \qquad (1.5)$$

Reactions 1.2 and 1.3 are the standard reactions for radiolysis of water. The presence of solutes, as in the case here, interferes with these reactions and, therefore, 1.2 and 1.3 are eliminated from the scheme herein discussed. Reaction 1.4 will occur and is dependent upon the dissolved oxygen content of the water. It is noteworthy that Reaction 1.4 interferes with 1.2 and also results in the conversion of the powerful reducing radical $H^{\cdot}$ into $HO_2^{\cdot}$, an oxidizing radical. Reaction 1.5 indicates the interaction of the TCE with the radiolysed water. All of the radicals previously mentioned react with the TCE, resulting in the same products. Reaction 1.5 is preferred over Reaction 1.4 in this system, since the dissolved-oxygen content is considerably lower than the TCE concentration. Reaction 1.5 is not reversible, since the trichloroethyl radical is stabilized by resonance and therefore has a lower free energy than the original $H^{\cdot}$ radical. The nonreversibility of Reaction 1.5 makes it the rate-determining step in the scheme and therefore sets the rate dependence of the dosimeter. Theory is here supported by the fact that no rate dependence has been observed at gamma dose rates from 1 r/hr to approximately 10^7 r/hr.

Since the sole interaction of gamma radiation with the dosimeter is Reaction 1.1, the energy dependence of the system is here established. The energy-transfer properties of water are very similar to those of tissue, and as a result, the dosimeter is exposed without shielding.

Reaction 1.4 could not by itself account for the marked oxygen dependence observed in the system. The following is proposed:

$$\begin{matrix} H & Cl \\ | & | \\ H-C-C^{\cdot} \\ | & | \\ Cl & Cl \end{matrix} + O_2 \longrightarrow \begin{matrix} H & Cl \\ | & | \\ H-C-C-O-O^{\cdot} \\ | & | \\ Cl & Cl \end{matrix} \qquad (1.6)$$

$$HO_2^{\cdot} + \begin{matrix} H & & Cl \\ & \diagdown\ \diagup & \\ & C=C & \\ & \diagup\ \diagdown & \\ Cl & & Cl \end{matrix} \longrightarrow \begin{matrix} H & Cl \\ | & | \\ {\cdot}C-C-O-O-H \\ | & | \\ Cl & Cl \end{matrix} \qquad (1.7)$$

In the event that oxygen is not present, the following occurs:

$$\begin{matrix} H & Cl \\ | & | \\ H-C-C^{\cdot} \\ | & | \\ Cl & Cl \end{matrix} + \begin{matrix} H & & Cl \\ & \diagdown\ \diagup & \\ & C=C & \\ & \diagup\ \diagdown & \\ Cl & & Cl \end{matrix} \longrightarrow \begin{matrix} H & Cl & H & Cl \\ | & | & | & | \\ H-C-C-C-C^{\cdot} \\ | & | & | & | \\ Cl & Cl & Cl & Cl \end{matrix} \qquad (1.8)$$

Reaction 1.8 is the first link in a chain reaction that produces a fibrous, inert polymer that is not acidic and will not be considered further here. The reaction product (1.6) may further react with TCE as shown below:

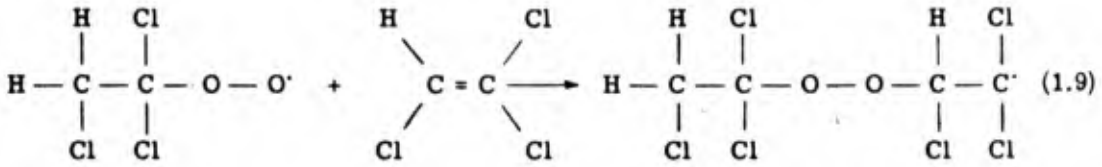

(1.9)

A chain reaction involving additional oxygen and TCE is possible as a continuation of Reaction 1.9; however, two component chains of this sort are virtually unknown. Radical-annihilation reactions are shown below:

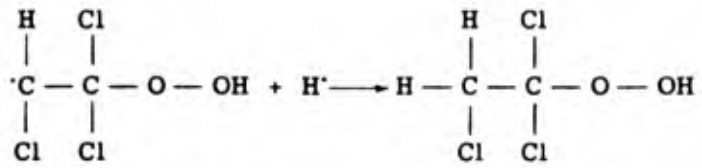

(1.10)

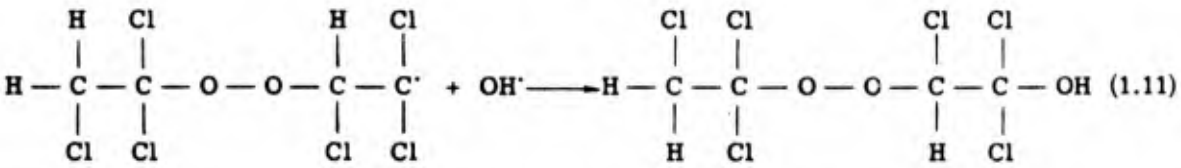

(1.11)

The following steps complete the reaction sequence and show production of the acidic products observed in the radiolysis:

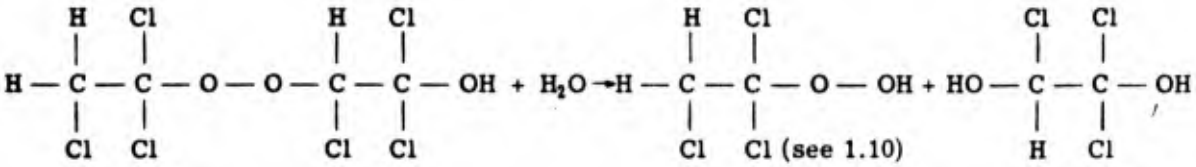

(1.12)

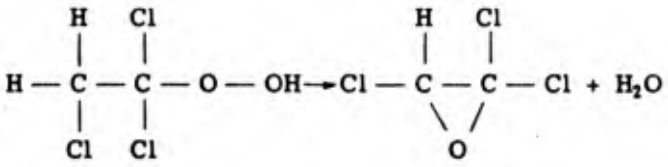

(1.13)

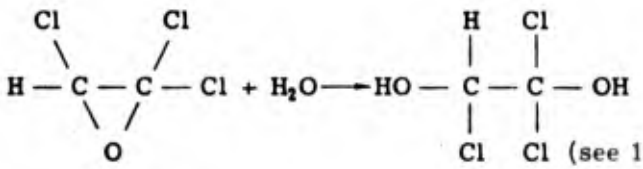

(1.14)

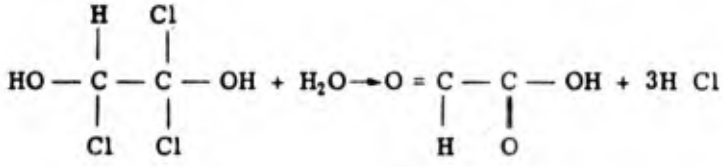

(1.15)

The two acids produced in Reaction 1.15 account for all of the acid produced. This and the fact that the hydrochloric acid concentration is three times that of glyoxylic acid have been experimentally demonstrated. Acid yields of the system for gamma radiation can be kept at values below 10^{-10} (moles/liter)/r and as high as 10^{-6} (moles/liter)/r.

Subsequent to Operation Hardtack, the TCE system was exposed to both fast and thermal neutrons in order to observe energy dependence and to obtain calibration values for use in calculating dose.

The results of exposure to fast neutrons is shown in Figure 1.1. The nomenclature Red/Silver Tubes and Blue/Silver Tubes are the color codes assigned to the two sets used at Shots Hamilton

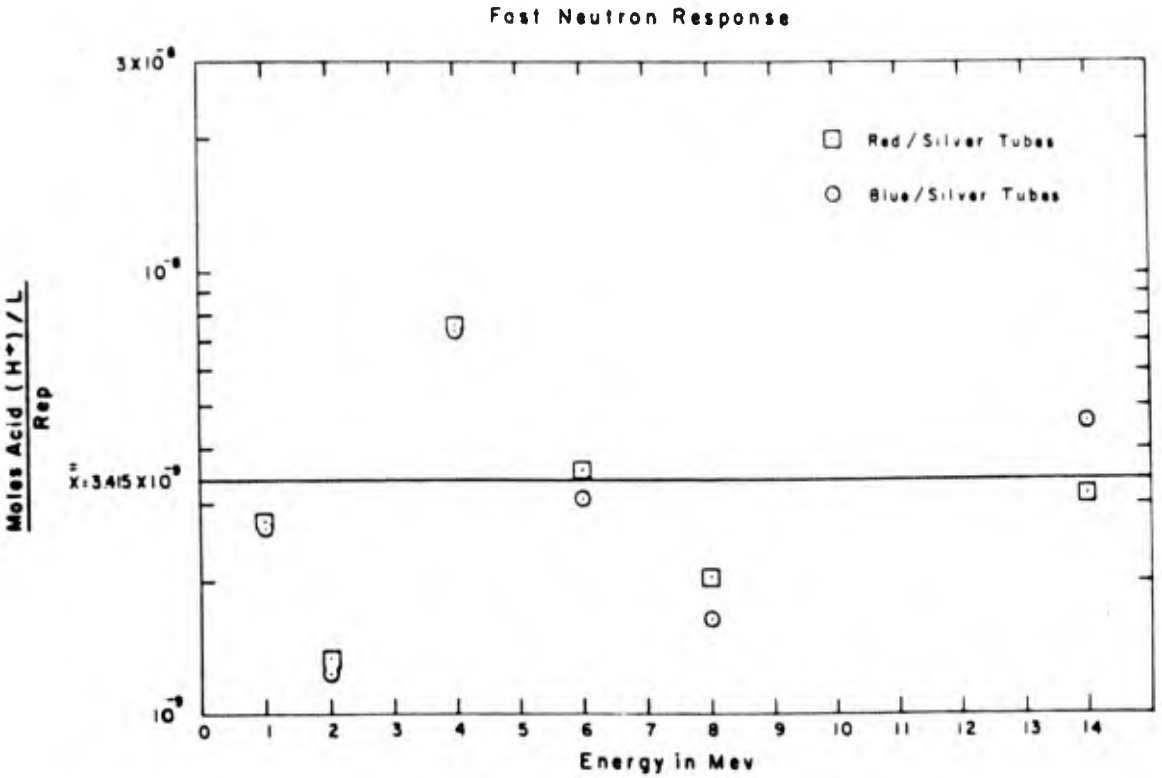

Figure 1.1 Fast-neutron response of the chemical dosimeter.

and Humboldt. Tubes from these sets were used in the studies of neutron-energy dependence. The composition of these tubes is described in Section 2.2.2 below. In Figure 1.1 the symbol $\bar{\bar{X}}$ refers to an average value. The curve shows acid production per unit dose as a function of neutron energy. Hurst's calculated values for (n/cm^2)/rep (References 9 and 10) based on single-collision theory were used. Since no energy dependence is demonstrated, it is valid to state that the means for neutron-energy transfer to the system is by proton recoil, which is the basis for Hurst's values in this energy region. Protons produce fairly dense ionization tracks in water. Ionic interactions in these tracks will be quite extensive and should account for virtually all the radiolysis products. This is strengthened by the evident lack of an oxygen effect. Ionic reactions rarely are affected by variations in oxygen content as are free-radical reactions. The absence of glyoxylic acid further substantiates this, because glyoxylic acid could be formed only by considerable oxygen interactions with the reaction intermediates.

Exposure of the system to thermal neutrons at the north thermal column of the water boiler reactor at LASL and use of the lithium extrapolation technique reveal a situation quite different from that observed for fast neutrons. Results are shown in Figure 1.2. The curve shows that the property of acid production per unit dose as a function of thermal-neutron flux is a function of lithium thickness. The positive slope of the curve indicates that there is a finite fast-neutron flux in the thermal column. This is of academic interest. Extrapolation of these lines to zero

lithium would indicate a true sensitivity. This extrapolated figure is in excellent agreement with fast-neutron response. However, the actual values at zero lithium thickness are quite different, being approximately 30 to 50 times higher than fast-neutron response values. This indicates an abnormally high sensitivity somewhere in the system. Since Hurst's values for $(n/cm^2)/rep$

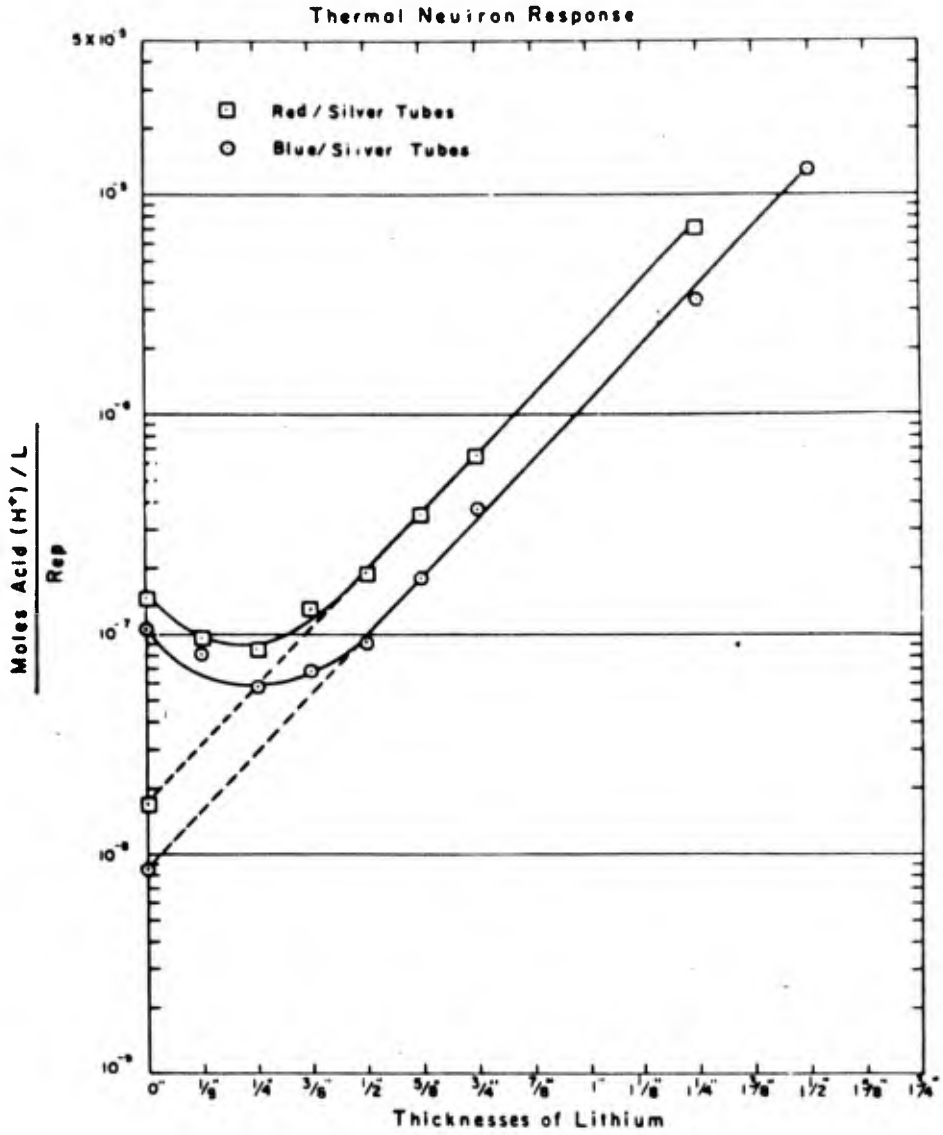

Figure 1.2 Thermal-neutron response of the chemical dosimeter.

were used here as they were for fast neutrons, a proper thermal response should be in agreement with values obtained for fast neutrons. The means for thermal-neutron energy transfer in water is by hydrogen capture to form deuterium with a subsequent emission of a 2.5-Mev gamma ray. One would then expect to observe thermal-neutron reactions with a marked similarity to gamma reactions in the system. No element is present in the TCE system to account for the observed supersensitivity. A review of the composition of the glass ampoules shows a B^{10} content of 0.2 percent. The thermal-neutron-capture cross section for B^{10} is approximately 4,000 barns resulting in B^{10} (n, α) Li^7. The lithium then emits a 400-kev gamma ray to drop to its ground state. The existence of this reaction around a system would cause an abnormally high sensitivity to thermal neutrons and would in fact make the differential-dosimetry system using only two tubes quite useless if measurements of gamma and neutron dose were to be made in the presence of thermal neutrons.

In the system described, two solutions were prepared at different oxygen contents. Irradiation of these two solutions produces acid. The nature of the radiation producing this acid can be determined by the use of the following equations:

$$X_1\gamma + Y_1 n + Z_1 n_{th} = T_1 \tag{1.16}$$

$$X_2\gamma + Y_2 n + Z_2 n_{th} = T_2 \tag{1.17}$$

The units are defined as:

X_1 Gamma-acid yield in Tube 1, $[H^+]/r$
X_2 Gamma-acid yield in Tube 2, $[H^+]/r$
Y_1 Fast-neutron acid yield in Tube 1, $[H^+]/rep$
Y_2 Fast-neutron acid yield in Tube 2, $[H^+]/rep$
Z_1 Thermal-neutron acid yield in Tube 1, $[H^+]/rep$
Z_2 Thermal-neutron acid yield in Tube 2, $[H^+]/rep$
T_1 Total acid observed in Tube 1, $[H^+]$
T_2 Total acid observed in Tube 2, $[H^+]$
γ Gamma dose received, r
n Fast-neutron dose received, rep
n_{th} Thermal-neutron dose received, rep

The constants X_1, X_2, Y_1, Y_2, Z_1, and Z_2 are determined by calibration with gamma, fast, and thermal neutrons. T_1 and T_2 are determined directly from the tubes exposed.

Chapter 2
PROCEDURE

2.1 OPERATIONS

Participation in Shots Quince and Fig during the Eniwetok Proving Ground (EPG) phase of Operation Hardtack consisted of attempts to measure neutron flux and dose versus ground range and to measure neutron, thermal, and gamma radiation up to an altitude of 1,500 feet.

During Shots Hamilton and Humboldt of the NTS phase, neutron radiation was measured with threshold detectors and chemical dosimeters. Gamma radiation was measured with the chemical dosimeters.

Pertinent information on the shots may be found in Table 2.1.

Each buoy station consisted of a Navy Mark 6 Model 3 mine case with concrete ballast and a tripodal steel-pipe tower. Figure 2.2 is a diagram of a buoy station with detectors installed. Figure 2.3 is a diagram of the buoy-station anchoring arrangement and is similar to that employed in Project 2.4 during the early phase of Operation Hardtack. If a buoy had sunk during the operation, the main cable lying on the lagoon floor would have been used in recovering it.

The detectors on the land line were recovered with a tractor, which pulled the cable to a noncontaminated area where the detectors were detached. Those at the stations on the buoy line were recovered with a DUKW.

A General Mills Aerocap balloon was instrumented and launched on the day prior to each shot. The launching was as late as possible to avoid the possible hazard of rain squalls and high winds.

The gamma and neutron detectors assigned to a station were fastened to a 4-foot length of $^{3}/_{16}$-inch wire rope that was attached with a halyard snap to a metal ring on the instrument cable of the balloon. The detectors were recovered by merely detaching the wire rope from the main cable.

The thermal detectors were wired directly to the metal rings on the instrument cable. It was necessary to run hard-wire connections from the thermal detectors to recorders located in the instrument shelters.

Information relative to the balloon instrument stations for Shots Quince and Fig is presented in Tables 2.3 and 2.4.

A detailed description of the balloons and their anchoring arrangements may be found in the Appendix.

All the neutron detectors were returned for analysis to the mobile laboratory trailer on Site Elmer; the gamma dosimeters were forwarded to the U. S. Army Signal Research and Development Laboratories (ASRDL), Fort Monmouth, New Jersey for analysis.

The thermal recordings were to have been analyzed on Site Elmer.

TABLE 2.2 STATION LOCATIONS, LAND AND WATER, SHOTS QUINCE AND FIG

Station Number	Slant Range	Azimuth
	yd	deg
241.01	100	143
241.02	200	143
241.03	300	143
241.04	400	143
241.05	500	143
241.06	600	143
241.07	700	143
241.08	800	143
241.09	900	143
241.10	30	143
242.01	30	233
242.02	100	233
242.03	247	233
242.04	344	233
242.05	444	233
242.06	603	233
242.07	816	233
242.08	1,039	233

TABLE 2.3 STATION LOCATIONS, BALLOON, SHOT QUINCE

Station Number	Slant Range	Detector
	ft	
1	120	Thermal *
2	150	Neutron †, gamma ‡, thermal
3	180	Thermal
4	210	Thermal
5	240	Thermal
6	250	Neutron, gamma, thermal
7	300	Thermal
8	380	Thermal
9	400	Neutron, gamma
10	600	Neutron, gamma
11	800	Neutron, gamma
12	1,100	Neutron, gamma
13	1,500	Neutron, gamma

* CWL thermistor.

† Threshold detectors (gold, plutonium, neptunium, uranium, and sulfur).

‡ NBS film badge.

TABLE 2.4 STATION LOCATIONS, BALLOON, SHOT FIG

Station Number	Height Above Ground	Ground Distance	Slant Range *	Detector
	ft	ft	yd	
1	100	350	121	Neutron †, gamma ‡
2	200	345	133	Neutron, gamma
3	395	335	173	Neutron, gamma
4	590	330	227	Neutron, gamma
5	785	325	283	Neutron, gamma
6	985	325	347	Neutron, gamma
7	1,180	325	410	Neutron, gamma

* Calculation of the slant ranges is described in the appendix. Quoted ranges are accurate to ± 20 feet.

† Threshold detectors (gold, plutonium, neptunium, uranium, and sulfur).

‡ NBS film badges.

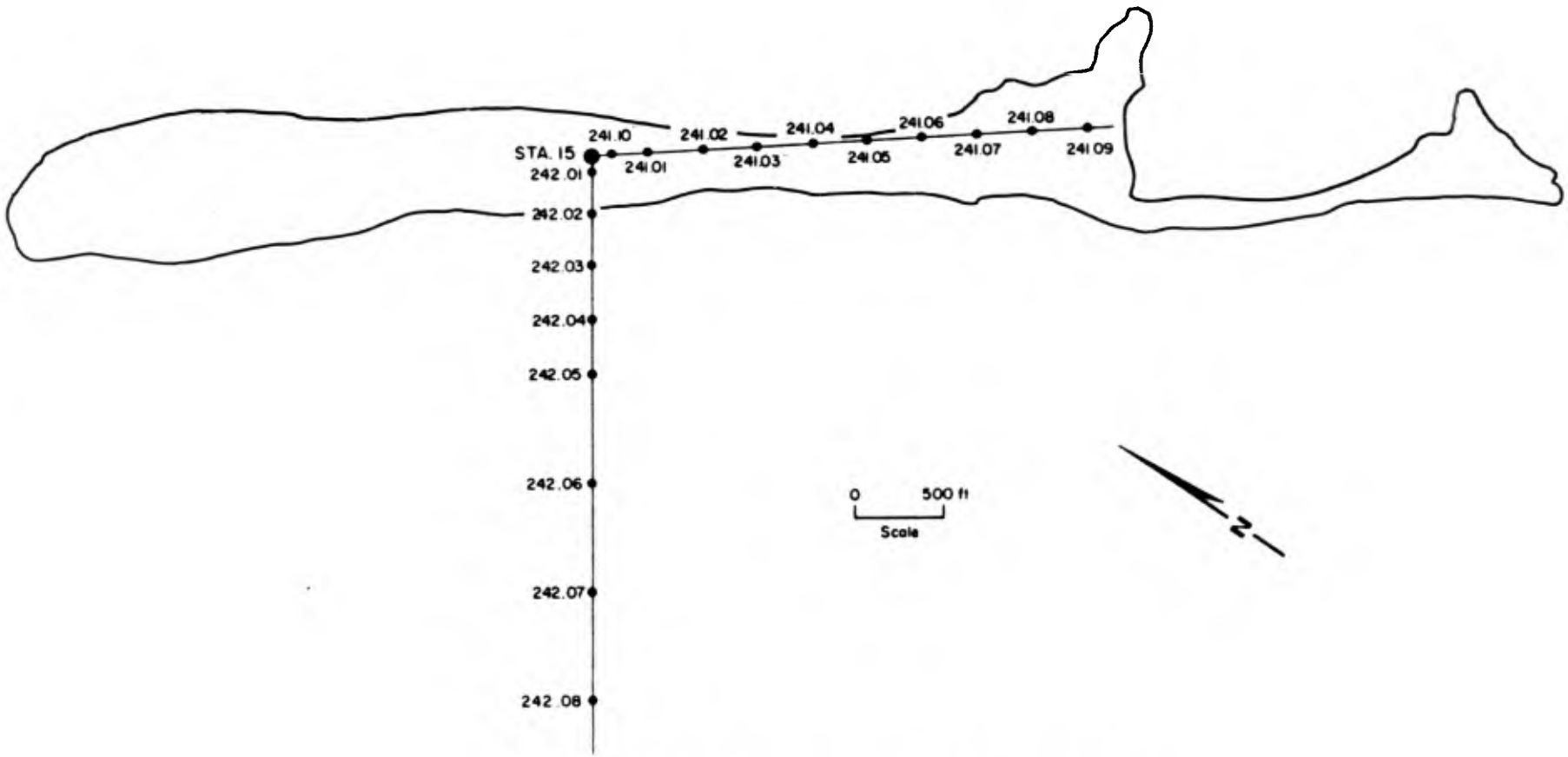

Figure 2.1 Land- and water-station layout, Shots Quince and Fig.

2.1.2 Shot Hamilton. Threshold detectors and chemical dosimeters were installed along two cable lines extending radially from ground zero at azimuths of 150 and 330 degrees. These lines were perpendicular to the long axis of the device, that is, along the axis of the expected maximum of neutron flux. These lines consisted of $\frac{3}{4}$-inch wire rope to which the detectors were

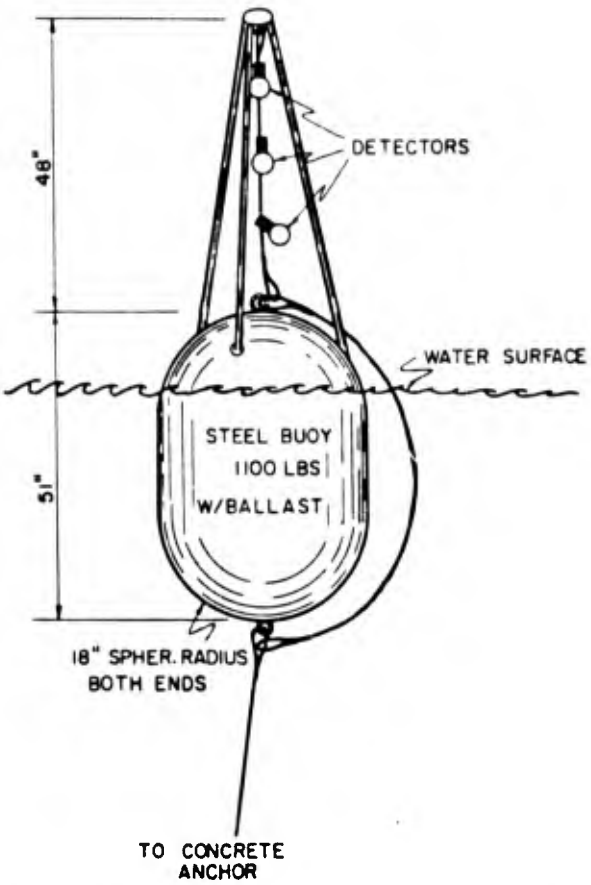

Figure 2.2 Diagram of buoy station with detectors installed.

attached with cable clamps and tape. Except for those in areas where the shock wave would probably have moved the wire rope, the detectors were elevated slightly so as to obtain a clear line of sight.

Chemical dosimeters were installed on goal-post stations located along the 150- and 330-degree azimuths, as well as along the 240-degree azimuth. Each goal-post station consisted of a steel rod that rested horizontally upon two vertical steel stakes driven into the ground.

Threshold detectors and chemical dosimeters were also installed inside M-48 tanks and armored personnel carriers (APC's), and others were exposed on steel stakes driven into the bottom of foxholes. The foxholes were open, two-thirds covered, or offset.

The open foxhole was merely a rectangular hole 7 feet long, 2 feet wide, and $4\frac{1}{2}$ feet deep, with a 6-inch high, 1-foot-wide berm around all but the end facing ground zero.

The two-thirds-covered foxhole was essentially an open foxhole in which the two-thirds of the opening nearest ground zero was covered with 6-by-6-inch timbers over which 1 foot of soil was placed.

The offset foxhole consisted of a rectangular hole 5 feet long, 7 feet deep, and 3 feet wide, with a firing step at the 4-foot level. At the 7-foot level, 90 degrees to the long axis of the foxhole, there was an offset 2 feet in diameter and $4\frac{1}{2}$ feet long. All but the firing-step portion of the foxhole was covered by 6-by-6-inch timbers and 1 foot of soil. The offset portion was covered by 5 feet of soil with a 1-foot overburden. A more complete description of the foxhole construction as well as information relative to the tanks and APC's may be found in Reference 14.

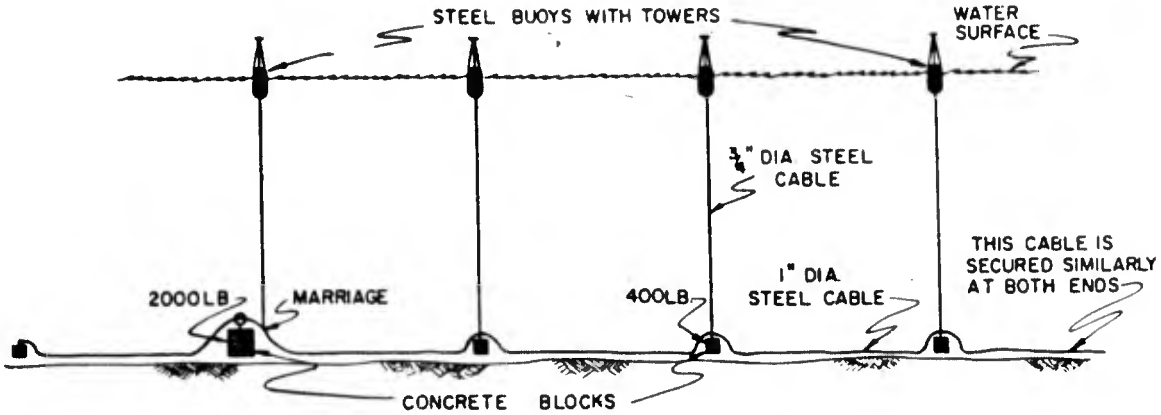

Figure 2.3 Buoy-station anchoring arrangement.

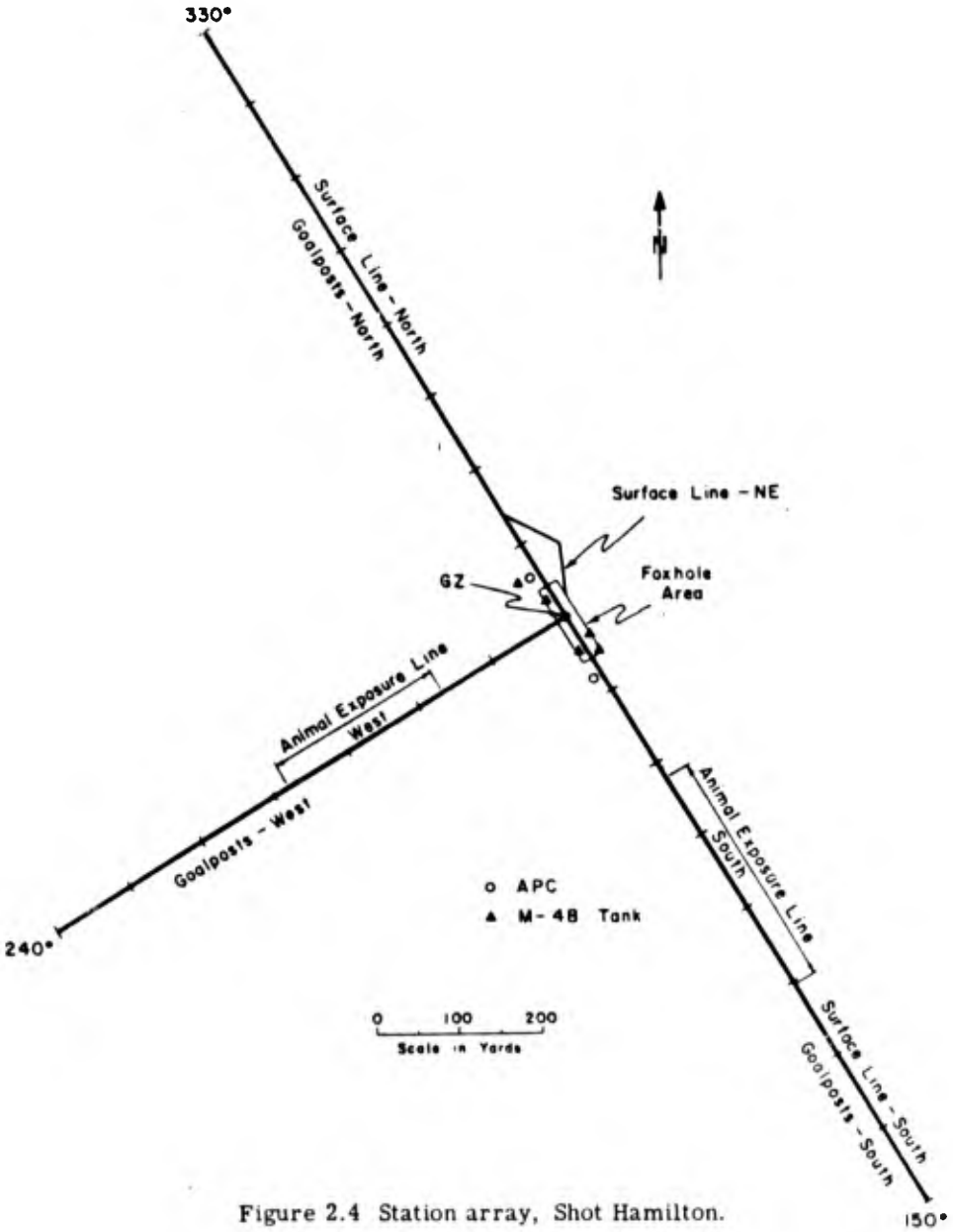

Figure 2.4 Station array, Shot Hamilton.

Ten additional sets of threshold detectors, which included gold, uranium, and sulfur detectors only, and approximately 125 chemical dosimeters were surgically inserted in the pigs by personnel of Project 4.2.

The locations of the threshold-detector system and the chemical-dosimeter system are shown in Tables 2.5 and 3.17, respectively. A plot plan of the station array is shown in Figure 2.4. Chemical dosimeters were used in three groups. Among the dosimeters exposed external to the animals, one set was numbered from 001 to 099, and a second from 1 to 200. Internal dosimeters were numbered from 1 to 150.

The detectors attached to the cable lines were recovered with 5-ton trucks, which pulled the cables to a radiologically safe area where the detectors were removed. Following recovery, the detectors were returned to the mobile laboratory trailer located in the forward area. The

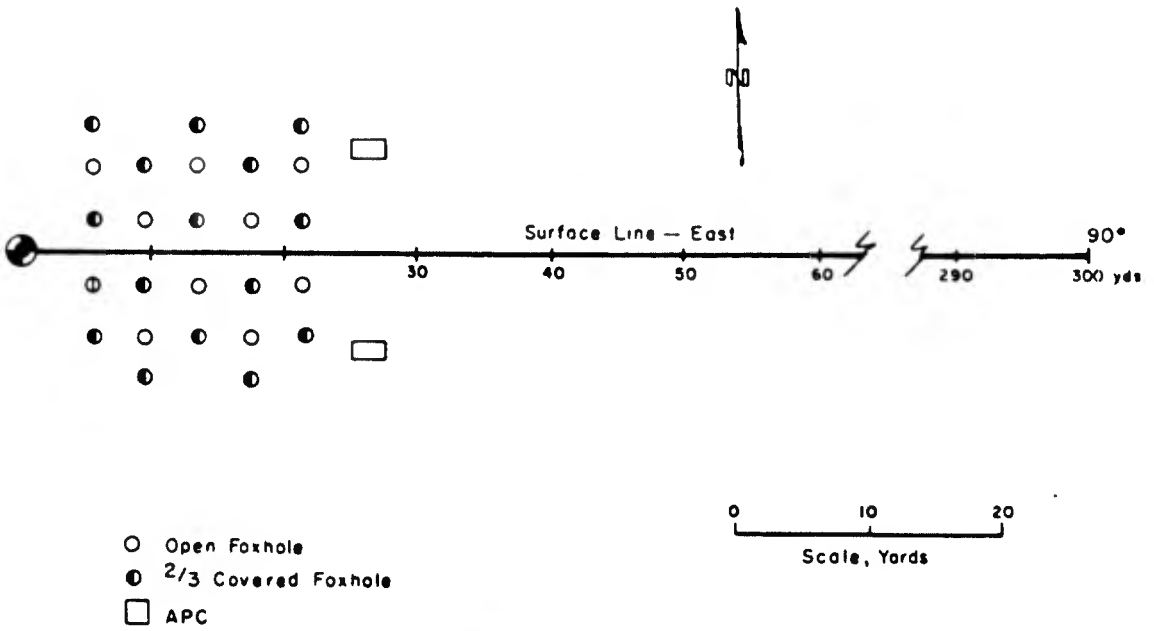

Figure 2.5 Station array, Shot Humboldt.

installation and recovery of all detectors exposed at goal-post stations, in foxholes, tanks, APC's, and pigs were accomplished by Project 4.2 personnel. For exact location of the detectors, reference should be made to the interim test report of that project (Reference 14).

All chemical dosimeters were returned to CWL for analysis.

2.1.3 Shot Humboldt. Threshold detectors and chemical dosimeters were installed along one cable line which ran generally east of ground zero.

Additional detectors were placed in open and two-thirds-covered foxholes and in two APC's located east of ground zero. These foxholes were similar to those constructed for Shot Hamilton; however, the animals were placed in aluminum liners inside the foxholes. The project instruments were laid across the tops of these liners.

The location of these detectors may be found in Tables 2.6 and 2.7. Figure 2.5 illustrates the station array for Shot Humboldt. Recovery and analysis procedures were the same as those following Shot Hamilton.

2.2 INSTRUMENTATION

2.2.1 Neutron Detectors. The threshold-detector technique was used to measure neutron flux. Gold, plutonium, neptunium, uranium, and sulfur were the specific detectors used. The reactions of interest have been previously listed.

TABLE 2.5 STATION LOCATIONS FOR THRESHOLD-DETECTOR SYSTEM, SHOT HAMILTON

Station Number	Azimuth	Slant Range	Type of Installation	Detectors
	deg	yd		
Basic Measurements:				
25 N	330	30.0	Surface	*
50 N	330	52.7	Surface	*
75 N	330	76.8	Surface	*
100 N	330	100	Surface	*
125 N	330	125	Surface	*
150 N	330	150	Surface	*
200 N	330	200	Surface	*
300 N	330	300	Surface	*
400 N	330	400	Surface	*
600 N	330	600	Surface	*
800 N	330	800	Surface	*
15 S	150	22.4	Surface	*
35 S	150	38.8	Surface	*
80 S	150	81.7	Surface	*
225 S	150	225	Surface	*
325 S	150	325	Surface	*
Project 2.12c Support Measurements:				
25 NE	350	30.0	Surface	*
50 NE	350	52.7	Surface	*
70 NE	350	72.0	Surface	*
Project 4.2 Support Measurements:				
10 SE	150	19.4	Offset foxhole	*
15 SE	150	22.4	Offset foxhole	*
33 SE	150	37.0	Tank	*, †
54 SE	150	56.5	Tank	*, †
47½ SW	150	50.3	Tank	*, †
80 SW	150	81.7	APC	*, †
7½ NE	330	18.3	Offset foxhole	*
12½ NE	330	20.8	Offset foxhole	*
20 NE	330	26.0	Open foxhole	*, †
32½ NE	330	36.5	Open foxhole	*, †
37½ NE	330	41.0	Open foxhole	*
40 NE	330	43.0	Open foxhole	*, †
32½ NW	330	36.5	Tank	*, †
57½ NW	330	60.0	APC	*, †
62½ NW	330	64.7	Tank	*, †

* Sulfur, gold, uranium, neptunium, and plutonium.
† Sulfur, gold, and uranium (surgically inserted in pigs).

TABLE 2.6 STATION LOCATIONS FOR THRESHOLD-DETECTOR SYSTEM, SHOT HUMBOLDT

Sulfur, gold, uranium, neptunium, and plutonium detectors were used at all stations.

Station Number	Slant Range	Type of Installation
	yd	
Basic Measurements:		
10	13.0	Surface
25	26.4	Surface
50	50.7	Surface
100	100	Surface
200	200	Surface
300	300	Surface
Project 4.2 Support Measurements:		
5 S	9.8	Open foxhole
5 N	9.8	½-covered foxhole
10 S	13.0	½-covered foxhole
10 N	13.0	Open foxhole
15 S	21.7	Open foxhole
15 N	21.7	½-covered foxhole
20 S	25.2	½-covered foxhole
20 N	25.2	Open foxhole
25 S	26.4	Open foxhole
25 N	26.4	½-covered foxhole
APC	33.0	APC
APC	33.0	APC

TABLE 2.7 CHEMICAL-DOSIMETER STATION LOCATIONS, SHOT HUMBOLDT

Station Number	Slant Range	Dosimeter Number
	yd	
Section I Dosimetry Stations External to Animals		
Surface (free-field) stations:		
10	13	195
25	26.4	183
50	50.7	144
100	100.0	180
200	200.0	175
300	300.0	207
Open foxhole stations:		
5 S	9.8	091
10 N	13.0	185
15 S	21.7	173
20 N	25.2	179
25 S	26.4	087
½-covered foxhole stations:		
5 N	9.8	083
10 S	13.0	190
15 N	21.7	139
20 S	25.2	143
25 N	26.4	156
Section II Dosimetry Stations Internal to Animals *		
APC, Number 66, SE		
1-66	28.0	129
6-66	29.5	118
7-66	29.2	124
8-66	29.0	125
19-66	32.4	126
APC, Number 70, NE		
1-70	27.7	133
9-70	29.8	140
10-70	30.0	131
11-70	30.3	141
20-70	33.0	137

* Five internally dosimetered animals were placed in each of two APC's. Although the same animals had been previously exposed on Shot Hamilton, they had sustained no dosage because of their location.

Gold was used as the slow-neutron detector. Duplicate disks of gold ½-inch in diameter and 10-mils thick were exposed. One disk was shielded with a 0.045-inch thickness of cadmium, while the other was bare. The difference in the induced activity of these two gold disks is proportional to the integrated neutron flux below 0.3 ev. This technique is referred to as the cadmium-difference technique.

The intermediate range of neutron energies, 10 kev to 3 Mev, was measured with three materials that fission when bombarded with neutrons. Since the thermal-neutron cross section for the first of these materials, Pu^{239}, is high, an artificial cross section had to be produced. This was accomplished by shielding the samples with B^{10}. In this manner, the effective threshold energy for Pu^{239} could be varied within limits by varying the amount of B^{10}. The threshold chosen for this event was 10 kev. The other materials, Np^{237} and U^{238}, fission only when bombarded with fast neutrons and have naturally occurring thresholds at 0.63 and 1.50 Mev, respectively. All of the fissionable materials were in the form of metal disks sealed in thin copper cups.

The fast neutrons were measured with the $S^{32}(n,p)P^{32}$ reaction. The sulfur detectors were molded pellets 1½ inch in diameter and ⅜ inch thick.

All of the samples were exposed in steel field holders that are completely described in Reference 7.

2.2.2 Chemical Dosimeters. The dosimeters consisted of two small glass vials, each containing approximately 1½ cm^3 of solution. The solution was prepared by saturating high-purity conductivity water (specific conductivity 2×10^6 minimum) with TCE in an atmosphere consisting of 99.99 percent helium plus 0.01 percent oxygen in one case and 99.30 percent helium plus 0.70 percent oxygen in the other. These atmospheres were achieved in a hermetically sealed, controlled-atmosphere chamber by continuous gas flow. The oxygen concentration was determined with a continuous-flow Beckman oxygen analyzer sensitive to 0.001 percent oxygen. The pH of the solution was set with unbuffered 0.001 NaOH prior to the filling and sealing of the ampoule. Before removal from the chamber, the ampoules were accurately filled and then sealed by using a resistance-heated coil of tungsten wire. Since the solution was unbuffered, the pH determinations were a valid measure of acid production upon irradiation. The pH was determined in the controlled-atmosphere chamber with a Beckman model GS pH meter and micro-electrodes. The sealed tubes are shown in Figure 2.6.

The dosimeters not placed in pigs were packaged in tin cans filled with vermiculite for protection from shock and rough handling. This package is shown in Figure 2.7. At stations closer than 100 yards, these cans were placed inside steel pipes and wired in place with cable. Dosimeters used internally were packaged in a condom and surgically placed in the pig without additional protective devices.

2.2.3 Gamma and Thermal Detectors. Total gamma dose was measured with NBS film badges. A complete discussion of these badges and their calibration may be found in Reference 15.

The thermal detector was the CWL thermistor calorimeter. A complete discussion of this detector and its calibration may be found in Reference 16.

2.3 DETECTOR ANALYSIS

2.3.1 Threshold Detectors. All the neutron detectors were returned for analysis to the mobile laboratory located on Site Elmer for the EPG phase and in the forward area for the NTS phase.

All gamma activity was measured by sodium iodide crystals, photomultiplier tubes, and standard counting equipment. The beta activity was measured with a plastic phosphor. This phosphor was attached to the photomultiplier tube in the same manner as was the sodium iodide crystal and was used with the same associated equipment, the only change being in the discriminator setting and the amplifier band width. A Co^{60} source was used as the monitoring medium.

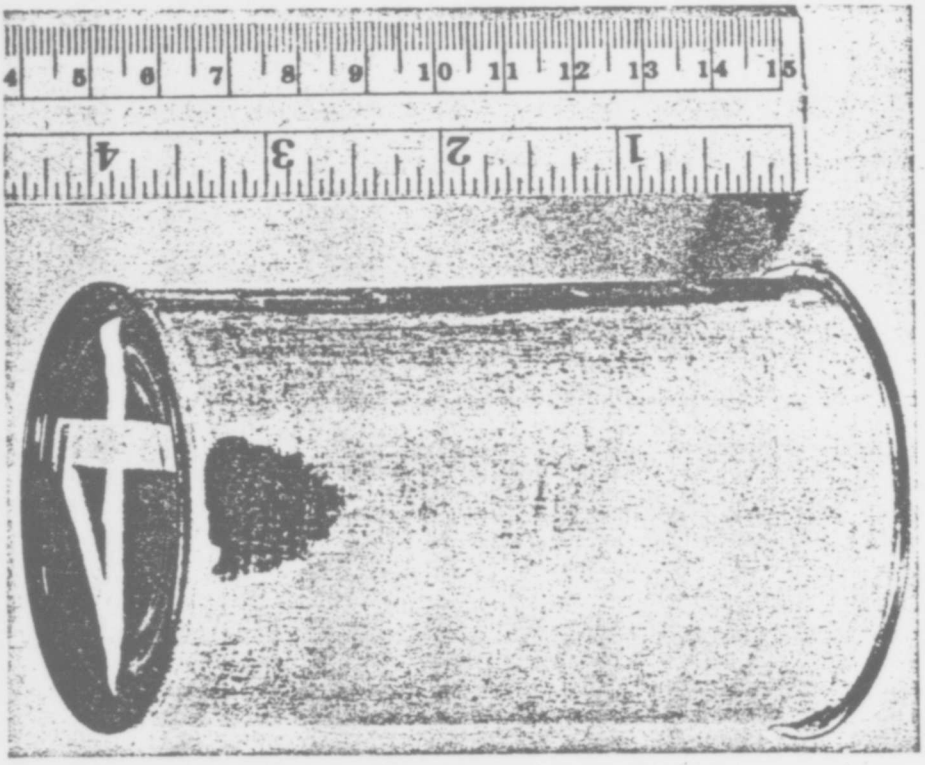

Figure 2.7 Chemical dosimeters packaged for external placement.

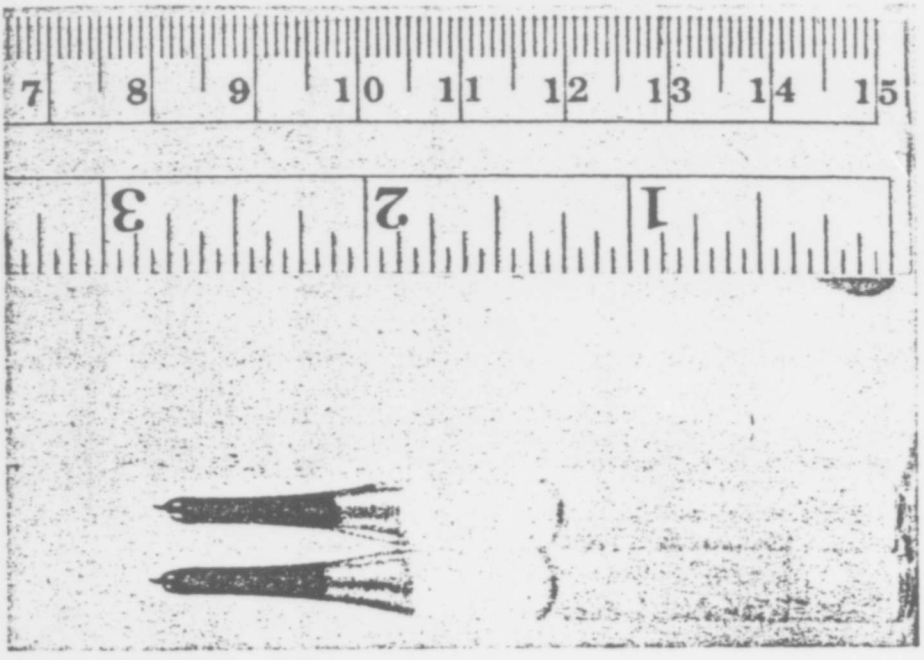

Figure 2.6 Chemical dosimeters.

A block diagram of this system is shown in Figure 2.8. This method has been used during several previous operations (References 5 and 6) and has proved to be accurate and convenient.

2.3.2 Chemical Dosimeters. After recovery, the detectors were returned to CWL for analysis. The tubes were placed in a controlled-atmosphere chamber where they were broken open and the pH of the liquid measured as described in Section 2.2.2. The pH change observed on

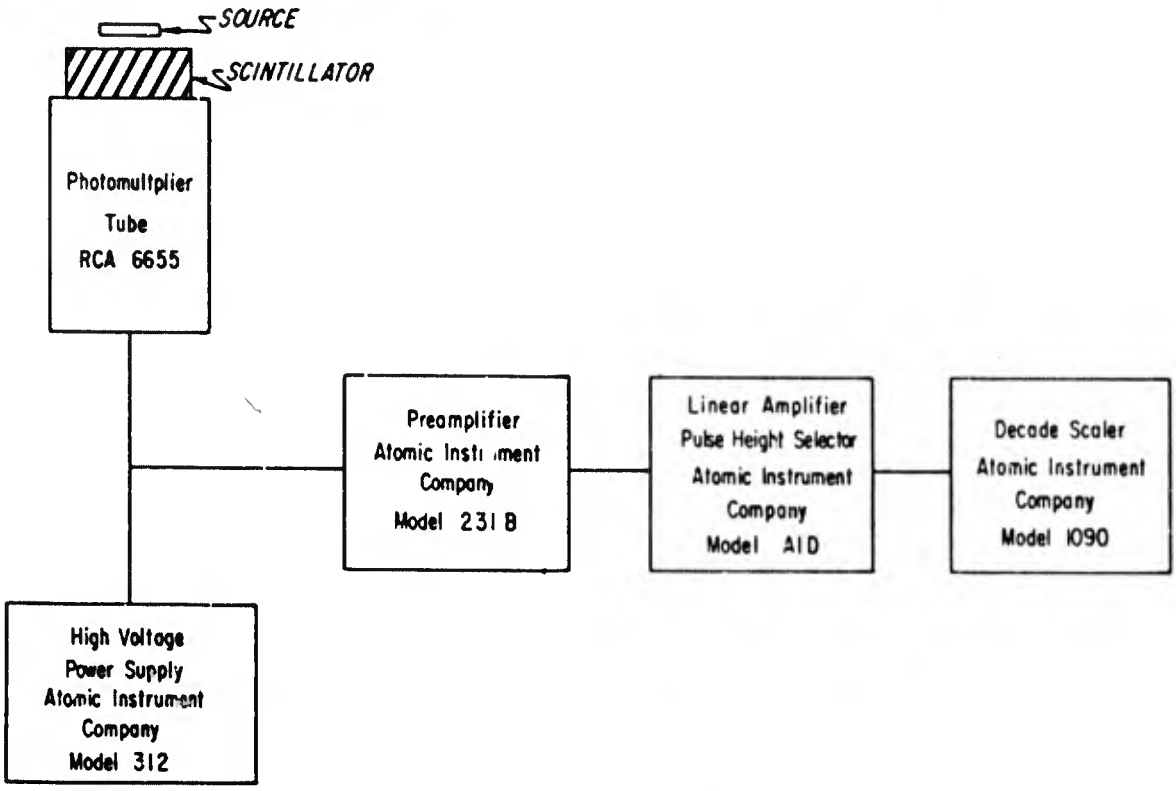

Figure 2.8 Block diagram of counting system.

exposure was a measure of the total acid produced. The quantity of total acid is represented by the terms T_1 and T_2 shown in Equations 1.16 and 1.17.

2.3.3 Gamma and Thermal Detectors. The gamma detectors were forwarded to ASRDL for analysis. The thermal recordings were to have been analyzed at Site Elmer by Project 8.7 personnel, with techniques described in Reference 16.

2.4 CALIBRATION OF DETECTORS

2.4.1 Threshold Detectors. Calibration of all detectors was accomplished at LASL, with the thermal column of the water-boiler reactor and the Cockroft-Walton accelerator as neutron sources. This calibration is described at length in Reference 17. The calibration numbers used for the fission detectors were calculated for the time of 10 hours after irradiation, while those for the gold and sulfur were calculated at exposure time and are as follows:

$$K_{Au} = 6.07 \times 10^5 \ \frac{n/cm^2}{count/min}$$

$$K_{Pu} = 2.21 \times 10^8 \left(\frac{n/cm^2}{count/min}\right)/gm$$

$$K_{Np} = 2.89 \times 10^8 \left(\frac{n/cm^2}{count/min}\right)/gm$$

$$K_U = 7.35 \times 10^8 \left(\frac{n/cm^2}{count/min}\right)/gm$$

$$K_S = 1.06 \times 10^7 \frac{n/cm^2}{count/min}$$

2.4.2 Chemical Dosimeters. The chemical dosimeters were calibrated with filtered X-ray and Co^{60} sources, with thermal neutrons at the water-boiler reactor at LASL, and with fast neutrons on the Van de Graaff and Cockroft-Walton accelerators at LASL. These calibrations resulted in the following values:

$X_1 = 15.7 \times 10^{-9}$ moles liter^{-1}/r

$X_2 = 5.4 \times 10^{-9}$ moles liter^{-1}/r

$Y_1 = 14.6 \times 10^{-9}$ moles liter^{-1}/rep

$Y_2 = 14.6 \times 10^{-9}$ moles liter^{-1}/rep

$Z_1 = 79.1 \times 10^{-9}$ moles liter^{-1}/rep

$Z_2 = 109.2 \times 10^{-9}$ moles liter^{-1}/rep

It should be noted that the differential-dosimetry technique is new and has not been investigated completely.

2.5 DATA REDUCTION

2.5.1 Neutron Flux. The neutron flux was calculated by multiplying the activity level of the samples (at the time after exposure at which the calibration number was calculated) by the calibration number. Except in the case of gold data, which only measures neutrons below 0.3 ev, the calculated flux figure signifies the total number of neutrons above the energy threshold of that particular detector. Therefore, a series of successive subtractions are necessary to obtain the number of neutrons between the various threshold energies.

2.5.2 Neutron Dose. Neutron dose was calculated from the neutron-flux values with the single-collision theory of dose contribution per neutron (Reference 9). The following equation was used in the calculation of neutron dose from the neutron-flux data:

$$\text{Dose (rep)} = [\, 1\,(N_{Pu} - N_{Np}) + 2.5\,(N_{Np} - N_U) + 3.2\,(N_U - N_S) + 3.9\,N_S\,]\,10^{-9} \qquad (2.1)$$

Where: N_{Pu} = flux above the Pu threshold

N_{Np} = flux above the Np threshold

N_U = flux above the U threshold

N_S = flux above the S threshold

The coefficients used were determined by taking the dose per neutron at the mean energy between the threshold energies of the successive detectors. No Au term is included in the equation above, because the dose contribution of the neutrons measured by the gold detector is insignificant.

2.5.3 Chemical Dosimetry. Gamma and neutron doses were determined with Equations 1.16 and 1.17.

At the time the experimental procedure was designed, the effect of thermal neutrons on the system was not yet known. It was thought that two terms would adequately define the total acid production. This would result in an equation with two unknowns. Solution of such a system

would require two simultaneous equations and hence two tubes, each at a different oxygen content. It is now evident that three terms are necessary for description of acid production. This would require three equations and three different oxygen content tubes. Since two equations cannot define three unknowns, the great majority of the chemical dosimeter stations did not yield any data. In those cases where gold foils were present at the same stations, a knowledge of thermal-neutron contribution exists and, therefore, the Z term in Equations 1.16 and 1.17 becomes known. These are the only stations at which doses are reported.

2.5.4 Film Badges. NBS film badges, for gamma-dose measurements, were processed and read by ASRDL.

Chapter 3
RESULTS

3.1 NEUTRON-FLUX RESULTS (THRESHOLD-DETECTOR TECHNIQUE)

All neutron-flux results are presented in units of total neutrons per square centimeter (n/cm^2) for each detecting material. As has been previously mentioned, the figures are the total number of neutrons above the effective threshold for all materials except gold. The effective thresholds of Pu^{239}, Np^{237}, U^{238}, and S are 10 kev, 0.63 Mev, 1.5 Mev, and 3.0 Mev, respectively. With gold, the results signify the number of neutrons between zero energy and the cadmium cutoff.

3.1.1 Shot Quince.

3.1.2 Shot Fig.

The results obtained from Shot Fig are presented in Table 3.1 for land stations, Table 3.2 for water stations, and Table 3.3 for balloon stations. Figures 3.1, 3.2, and 3.3 are representations of neutron flux times slant distance squared versus slant distance for land, water, and balloon stations, respectively.

3.1.3 Shot Hamilton.

The results obtained from Shot Hamilton surface stations are presented in Table 3.4, and plotted in Figure 3.4 as neutron flux times slant distance squared versus slant distance. Table 3.5 lists the measurements made in support of Program 4.2, and Table 3.6 presents the results of detectors surgically inserted in pigs.

No uranium fluxes are quoted in Table 3.6, because the uranium detectors had not been shielded against thermal neutrons and consequently it was impossible to determine an adequate calibration number for these detectors.

3.1.4 Shot Humboldt.

Results from Shot Humboidt surface stations are presented in Table 3.7, and measurements made in support of Program 4.2 are listed in Table 3.8. Figure 3.5 is a representation of neutron flux times slant distance squared versus slant distance.

3.2 NEUTRON-DOSE RESULTS (THRESHOLD-DETECTOR TECHNIQUE)

Neutron-dose data were calculated from the flux data by using Equation 2.1. In cases where neptunium-flux data were lacking, the dose data were calculated from the following equation:

$$\text{Dose (rep)} = [\,1.8\,(N_{Pu}-N_U) + 3.2\,(N_U-N_S) + 3.9\,N_S\,] \times 10^{-9} \qquad (3.1)$$

Where: N_{Pu} = flux above Pu threshold

N_U = flux above U threshold

N_S = flux above S threshold

Neutron-dose information for Shots Hamilton and Humboldt is presented for two sets of meteorological conditions: (1) as measured for the conditions shown in Table 3.9 and (2) as corrected to the conditions of a relative air density of unity (in units of 1.22×10^{-3} gm/cm^3, the density of average atmospheric air at 1,013-mb pressure and 15 C temperature). Because the interpretation of previous experimental data has indicated that the perturbations of the flux due to atmospheric water vapor are much less than the error in the measurements themselves, the

Pages 34 thru 41 Deleted.

effect of water-vapor content was neglected. Thus, the corrected data for Shots Hamilton and Humboldt may be compared directly with data for the various devices detonated at EPG, since the meteorological conditions there are very similar to the standard conditions chosen for unity air density.

The above-mentioned corrections were made by means of the following formulas and relations:

$$\bar{\rho} = 0.284\ P/T \tag{3.2}$$

If

$$\bar{\rho}_1 R_1 = \bar{\rho}_2 R_2 \tag{3.3}$$

and since

$$\phi_2 = (R_1/R_2)^2\ \phi_1$$

then

$$\phi_2 = (\bar{\rho}_2/\bar{\rho}_1)^2\ \phi_1 \tag{3.4}$$

Where: $\bar{\rho}$ = relative air density
P = ambient atmospheric pressure, mb
T = ambient atmospheric temperature, deg K
R = slant range from device to detector, yd
ϕ = neutron dose, rep

Equation 3.2 was used to calculate the relative air densities for the conditions under which each device was detonated.

3.2.1 Shot Fig. Neutron-dose information is listed in Tables 3.10, 3.11, and 3.12 for land, water, and balloon stations, respectively. The dose results for the land, water, and balloon stations are presented as dose times slant distance squared versus slant distance in Figure 3.6 and as dose versus slant distance in Figure 3.7.

3.2.2 Shot Hamilton. Neutron-dose data obtained from surface stations are listed in Table 3.13. Table 3.14 lists the measurements made in support of Program 4.2. Figures 3.8 and 3.9 are representations of the dose results at the surface stations.

Pages 43 & 44 Deleted.

TABLE 3.17 GAMMA- AND NEUTRON-DOSE RESULTS (CHEMICAL DOSIMETRY), SHOT HAMILTON

Station Number	Slant Range	Dosimeter Number		Dose	
				Gamma	
	yd			r	
Section I Dosimetry Stations External to Animals					
Surface (free-field)* stations:					
25 N	30.0	13		†	
		17		†	
50 N	52.7	11		†	
		61		901	
		68		228	
		67		994	
			Average	708	Average
75 N	76.8	56		910	
		72		892	
		85		893	
		95		888	
			Average	896	Average
100 N	100	71		889	
		74		374	
		77		734	
		81		851	
		99		799	
			Average	729	Average
125 N	125	55		†	
		78		704	
		87		800	
		91		336	
		93		412	
			Average	563	Average
150 N	150	51		843	
		65		944	
		67		†	
		98		872	
			Average	886	Average
200 N	200	58		537	
		64		906	
		75		†	
			Average	722	Average
300 N	300	66		1,100	
		83		805	
		86		†	
		92		910	
			Average	938	Average
400 N	400	52		‡	
		57		‡	
		62		‡	
		63		‡	
		73		‡	
		96		‡	
		081		‡	
		086		‡	
		089		‡	
		092		‡	
		093		‡	
		095		‡	

TABLE 3.17 CONTINUED

Station Number	Slant Range	Dosimeter Number		Dose Gamma	
	yd			r	
600 N	600	53		†	
		76		594	
		79		1,002	
		88		834	
			Average	810	Average
800 N	800	59		1,049	
		82		929	
		84		968	
		89		216	
			Average	791	Average
15 S	22.4	100		‡	
35 S	38.8	97		‡	
		99		‡	
80 S	81.7	101		‡	
225 S	225	102		‡	
325 S	325	103		‡	
Goal post § west (240 degrees) stations:					
100 W	100	060		763	
I	170	008		‡	
		114		‡	
II	185	050		‡	
		125		‡	
200 W	200	123		915	
III	200	119		†	
		120		†	
IV	215	126		‡	
		132		‡	
VI	245	129		‡	
		130		‡	
VIII	275	152		‡	
		158		‡	
300 W	300	113		718	
X	305	147		‡	
		153		‡	
XII	335	127		‡	
		146		‡	
XIV	365	157		‡	
		170		‡	
XV	380	133		‡	
		163		‡	
400 W	400	106		814	
500 W	500	112		587	
600 W	600	113		717	
700 W	700	124		‡	

TABLE 3.17 CONTINUED

Station Number	Slant Range	Dosimeter Number	Dose Gamma
	yd		r
Goal post south (150 degrees) stations:			
100 S	100	045	594
200 S	200	122	622
I	225	128	‡
		131	‡
II	245	159	‡
		165	‡
III	265	136	‡
		166	‡
IV	285	134	‡
		164	‡
300 S	300	117	548
VI	325	137	‡
		160	‡
VIII	364	149	‡
		154	‡
400 S	400	115	790
X	405	155	‡
		191	‡
XII	445	138	‡
		167	‡
XIV	485	171	‡
		172	‡
500 S	500	116	753
XV	505	135	‡
		148	‡
600 S	600	121	484
XVI	650	108	‡
		141	‡
700 S	700	111	‡
XVII	750	107	‡
		142	‡
800 S	800	105	‡
Goal post north (330 degrees) stations:			
25 N	30.0	056	537
50 N	52.7	054	806
75 N	76.8	066	590
100 N	100	069	556
125 N	125	110	573
150 N	150	109	589
175 N	175	104	‡

TABLE 3.17 CONTINUED

Station Number	Slant Range	Dosimeter Number	Dose Gamma
	yd		r
Stations inside vehicles ¶:			
67 Tank NW	32.5	003	580
68 Tank SE	33.0	029	606
69 Tank SW	47.5	004	‡
70 Tank SE	54.0	009	563
66 APC NW	57.5	002	583
65 Tank NW	62.5	005	718
71 APC SW	80.0	007	418
Open-foxhole stations:			
14 SW	15.0	052	‡
62 NE	15.0	027	‡
40 NW	17.5	059	‡
26 NE	17.5	021	‡
58 NE	20.0	058	805
10 SW	20.0	079	‡
22 SE	22.5	051	‡
23 SE	22.5	076	‡
21 SE	22.5	035	‡
54 NE	25.0	046	‡
55 NE	25.0	062	‡
56 NE	25.0	053	‡
19 SE	27.5	073	‡
20 SE	27.5	077	‡
5 SW	30.0	041	‡
6 SW	30.0	028	‡
18 SE	32.5	037	†
49 NE	32.5	030	616
48 NE	35.0	040	‡
4 SW	35.0	038	‡
17 SE	37.5	080	‡
47 NE	37.5	078	651
46 NE	40.0	017	799
3 SW	40.0	006	‡
1 SW	55.5	070	‡
2 SW	55.5	067	‡
⅔-covered foxholes:			
29 SE	12.5	061	‡
28 SE	12.5	071	‡
43 NW	12.5	020	‡
41 NW	15.0	049	‡
42 NW	15.0	015	‡
13 SW	15.0	019	‡
59 NE	17.5	014	‡
60 NE	17.5	025	‡
12 SW	17.5	074	‡
39 NW	20.0	012	‡
24 SE	20.0	068	‡
25 SE	20.0	043	‡
36 NW	22.5	016	‡
37 NW	22.5	063	‡

TABLE 3.17 CONTINUED

Station Number	Slant Range	Dosimeter Number	Dose Gamma
	yd		r
57 NE	22.5	031	‡
7 SW	25.0	055	‡
8 SW	25.0	032	‡
9 SW	25.0	023	‡
51 NE	27.5	022	‡
52 NE	27.5	072	‡
53 NE	27.5	065	‡
34 NW	30.0	064	‡
35 NW	30.0	010	‡
50 NE	30.0	048	‡
32 NW	40.0	047	‡
33 NW	40.0	034	‡
Offset-foxhole stations:			
31 SE	5.0	057	‡
45 NW	5.0	011	‡
64 NE	7.5	026	524
16 SW	7.5	033	‡
30 SE	10.0	024	729
44 NW	10.0	036	‡
63 NE	12.5	039	614
15 SW	12.5	075	‡
27 SE	15.0	042	‡
61 NE	15.0	044	‡
38 NW	20.0	013	‡
11 SW	20.0	018	‡
Section II Dosimetry Stations Internal to Animals			
Open-foxhole stations:			
62 NE	15.0	56	‡
26 SE	17.5	50	‡
10 SW	20.0	43	‡
58 NE	20.0	136	538
21 SE	22.5	25	—
23 SE	22.5	19	‡
54 NE	25.0	9	‡
55 NE	25.0	1	‡
56 NE	25.0	15	‡
19 SE	27.5	36	‡
20 SE	27.5	139	‡
5 SW	30.0	42	‡
18 SE	32.5	13	‡
49 NE	32.5	107	†
4 SW	35.0	59	‡
48 NE	35.0	3	‡
17 SE	37.5	40	‡
47 NE	37.5	17	‡
3 SW	40.0	81	†
46 NE	40.0	110	570
1 SW	55.0	41	‡
2 SW	55.0	70	‡

TABLE 3.17 CONTINUED

Station Number	Slant Range	Dosimeter Number	Dose Gamma
	yd		r
⅔-covered-foxhole stations:			
28 SE	12.5	30	‡
29 SE	12.5	57	‡
43 NW	12.5	35	‡
13 SW	15.0	68	‡
42 NW	15.0	39	‡
12 SW	17.5	21	‡
59 NE	17.5	49	‡
24 SE	20.0	29	‡
25 SE	20.0	60	‡
39 NW	20.0	38	‡
36 NW	22.5	2	‡
37 NW	22.5	18	‡
57 NE	22.5	31	‡
7 SW	25.0	63	‡
8 SW	25.0	135	‡
9 SW	25.0	27	‡
51 NE	27.5	23	‡
52 NE	27.5	4	‡
53 NE	27.5	26	‡
34 NW	30.0	7	‡
35 NW	30.0	46	‡
50 NE	30.0	47	‡
32 NW	40.0	62	‡
33 NW	40.0	22	‡
Offset-foxhole stations:			
31 SE	5.0	16	‡
45 NW	5.0	20	‡
64 NE	7.5	5	717
30 SE	10.0	10	‡
15 SW	12.5	34	†
63 NE	12.5	14	585
27 SE	15.0	12	968
61 NE	15.0	51	†
38 NW	20.0	44	‡
Vehicle stations:			
67 Tank NW	32.5	123	926
68 Tank SE	33.0	120	887
69 Tank SW	47.5	112	73
70 Tank SE	54.0	102	619
66 APC NW	57.5	109	590
65 Tank NW	62.5	130	1,854
71 APC SW	80.0	105	531
Animal-exposure line, west (240 degrees):			
I	170	118	‡
		140	‡
		141	‡
II	185	124	‡
		129	‡
		137	‡

TABLE 3.17 CONTINUED

Station Number	Slant Range	Dosimeter Number	Dose
			Gamma
	yd		r
III	200	125	‡
		126	‡
		133	‡
IV	215	11	‡
		54	‡
		131	‡
VI	245	95	‡
		100	‡
VIII	275	32	‡
		58	‡
		82	‡
X	305	64	‡
		71	‡
		73	‡
XII	335	67	‡
		75	‡
		97	‡
XIV	365	53	‡
		69	‡
		94	‡
XV	380	8	‡
		24	‡
		85	‡
Animal-exposure line, south (150 degrees):			
I	225	80	‡
		104	‡
		122	‡
II	245	55	‡
		101	‡
		115	‡
III	265	86	‡
		89	‡
		103	‡
IV	285	90	‡
		116	‡
		128	‡
VI	325	72	‡
		77	‡
		79	‡
		93	‡
VIII	365	98	‡
		106	‡
		127	‡

TABLE 3.17 CONTINUED

Station Number	Slant Range	Dosimeter Number	Dose
			Gamma
	yd		r
X	405	91	‡
		110	‡
		134	‡
XII	445	113	‡
		114	‡
		121	‡
XIV	485	87	‡
		117	‡
		132	‡
XV	505	88	‡
		108	‡
		119	‡

* Surface, north, and south cable lines placed by Project 2.12a personnel. Stations coincided with threshold-detector stations.

† Dosimeter broken or missing.

‡ No thermal-neutron data available, therefore, dose cannot be calculated.

§ Goal posts and crossbars on stakes placed by Project 4.2 personnel.

¶ Vehicles and foxholes. All dosimeters placed and recovered by Project 4.2 personnel.

TABLE 3.18 GAMMA- AND NEUTRON-DOSE RESULTS (CHEMICAL DOSIMETRY), SHOT HUMBOLDT

Dosimeter Position	Slant Range	Dosimeter Number	Dose
			Gamma
	yd		r
Surface (Free-Field) Stations:			
50	50.7	144	3,440
100	100.0	180	2,109
200	200.0	175	531
300	300.0	207	629
Open-Foxhole Stations:			
20 N	25.2	179	3,607
25 S	26.4	087	1,581
⅔-Covered Foxhole Stations:			
5 N	9.8	083	1,892
10 S	13.0	190	2,011
15 N	21.7	139	2,080
20 S	25.2	143	3,615
25 N	26.4	156	9,513

Pages 54 thru 58 Deleted.

3.2.3 Shot Humboldt. Tables 3.15 and 3.16 list the neutron-dose results from Humboldt surface stations, and Program 4.2 support measurements, respectively. Figures 3.10 and 3.11 are representations of the surface-dose information.

3.3 NEUTRON AND GAMMA MEASUREMENTS (CHEMICAL-DOSIMETER SYSTEM)

Gamma and neutron dose for those locations at which thermal-neutron doses were available are listed in Tables 3.17 and 3.18 for Shots Hamilton and Humboldt, respectively.

3.4 GAMMA AND THERMAL MEASUREMENTS

The gamma-dose information from NBS film badges for Shot Fig balloon and land stations is listed in Tables 3.19 and 3.20, and represented in Figure 3.12.

As has been previously mentioned, the thermal detectors were eliminated in order to reduce the lift requirements on the balloon.

Chapter 4
DISCUSSION

4.1 THRESHOLD-DETECTOR MEASUREMENTS—NEUTRON FLUX

4.1.1 Data Reliability. The early recovery of the detectors from all three shots enhanced the degree of reliability of the fission threshold-detector data. All detectors were recovered and measurements begun by H + 1 hour for Shot Fig and H + 1½ hours for Shots Hamilton and Humboldt. The measured decay of each sample followed the known decay rates for the nuclides under consideration. A general discussion of the reliability of data obtained with the threshold-detector system is contained in References 6 and 7.

Page 61 deleted.

4.3 FILM-BADGE MEASUREMENTS—GAMMA DOSE

Under ideal conditions, the accuracy of data resulting from the use of the film-dosimeter system is given as ±30 percent.

Figure 3.12 shows that the gamma dose recorded at the balloon stations was higher by factors of two to three (increasing with range) than predicted doses and doses measured on the ground by Project 2.9. This factor of two difference was also observed by Project 2.12b at close-in

TABLE 4.1 NEUTRON DOSE PER UNIT YIELD FOR SHOTS FIG, HAMILTON, HUMBOLDT, AND TM 23-200 PREDICTION

Slant Distance	Shot		TM 23-200
	Hamilton *	Humboldt *	
yd	rep/kt	rep/kt	rep/kt
25	1.20×10^7 ‡	1.38×10^7 ‡	§
30	1.10×10^7 ‡	9.20×10^6 ‡	§
50	4.90×10^6 ‡	3.30×10^6 ‡	§
100	8.80×10^5 ‡	8.80×10^5 ‡	§
200	1.40×10^5 ‡	1.60×10^5 ‡	§
300	4.00×10^4 ‡	4.15×10^4	§
400	1.28×10^4 †	1.40×10^4 †	§
500	4.50×10^3 †	4.70×10^3 †	3.60×10^3
600	1.80×10^3 †	1.80×10^3 †	2.00×10^3
700	7.60×10^2 †	7.80×10^2 †	1.10×10^3
800	3.30×10^2 †	3.50×10^2 †	6.30×10^2
900	1.50×10^2 †	1.60×10^2 †	3.60×10^2
1,000	7.10×10^1 †	7.50×10^2 †	2.10×10^2

* Corrected to a relative air density of 1.0 (see Section 3.2).

† Extrapolated values.

‡ Interpolated values.

§ No predictions available for these points.

ground stations for Shots Hamilton and Humboldt which were low air bursts of devices similar to Shot Fig. Therefore, at close-in stations the interchange of source and detector (airborne measurement station and surface burst versus surface measurement station and air burst) gave consistent factors. At greater distances, the factors diverged, becoming higher for the balloon measurements at Shot Fig and lower for the air-burst measurements. This discrepancy can be explained by the geometry of the balloon stations. The vertical string of detectors was offset 120 yards from ground zero. The fireball and cloud rose vertically with high initial velocity, passing within about the same distance from each detector during transit. The slant distance of Figure 3.12 would apply for nitrogen-capture gamma radiation (during the first few milliseconds) but would not apply for fission-product radiation in the ascending source. The equalizing of the cloud-to-detector distance during the ascent of the cloud-fission products would result in readings that would be too high. Therefore, balloon measurements would be applicable for situations only where the ascending cloud would cause only minor changes in slant distances.

For a more complete discussion of the gamma data see Reference 15.

4.4 CHEMICAL DOSIMETRY

The results obtained at Shots Hamilton and Humboldt indicate that the procedure employed for the differential dosimetry measurements was improperly designed. Very little data of any kind was obtained, and the data that was obtained appears to be of little or no value. At the time,

virtually nothing was known about the neutron response of the system. Although there was small probability of obtaining useful data, the attempt was made because of the impending test ban. The personnel of Project 4.2, for whom the measurements were made, were cognizant of this fact. It should be further stated that, because of the very large number of individual measurements desired by Project 4.2, chemical dosimetry was the only technique available to them, the number of available threshold detectors being quite limited.

The lack of precision in the chemical-dosimeter measurements is due largely to the limited time in which the system had to be prepared. Careful quality control and precise testing had to be sacrificed in order to make the equipment available on time.

Subsequent laboratory work has shown that differential dosimetry, as described, is a feasible and relatively simple method for determining gamma and neutron dose when both radiations are present.

Page 64 Deleted.

Appendix A
AEROCAP BALLOON OPERATIONS

A.1 OBJECTIVES

The objectives of the balloon flights were to carry 300 to 400 pounds of instrumentation to various levels up to 1,500 feet above the terrain and to position this instrumentation at a point where it would be virtually unaffected by winds up to 30 knots.

A.2 BACKGROUND

Until 1956, the most common balloon in use was the natural-shape type, so called because the gas inside the plastic envelope was allowed to produce a shape with no circumferential stress.

During 1956, there was a requirement for balloons that would maintain fixed positions when tethered at low altitudes. The natural-shape balloons did not meet the requirement, because their drag coefficient was high. This led to production of the brute-force balloon, so called because the static free lift was equal to several times the pay load. However, this type proved to be very inefficient both in the use of helium and in the cost of ground facilities.

At this time, the engineers at General Mills, Inc., decided that the solution to the problem would be a balloon that produced aerodynamic lift with minimum aerodynamic drag. In order to minimize the lateral excursion of the balloon in flight and therefore fix its position in mid-air, the aerodynamic lift had to be greater than the drag. A balloon with these characteristics was designed by General Mills, Inc., and called the Aerocap.

A.3 DESIGN CONCEPT

For optimum design, the following properties had to be obtained: low drag coefficient, high volume efficiency, lightweight construction, and good aerodynamic performance. Drag coefficients in several shapes and fineness ratios had been defined in wind-tunnel tests by the National Advisory Committee for Aeronautics. The fineness ratio is defined as the length of the balloon divided by the maximum diameter. As the fineness ratio increases, the drag coefficient decreases, but the volume efficiency also decreases and at a greater rate. It was discovered that the Navy, Class C, shaped balloon, with a 3-to-1 fineness ratio, met the aerodynamic requirements very closely. This shape had an inherent stability feature, because the center of buoyancy was located forward of the center of gravity. This location of force assisted in diminishing the upsetting moments created by vertical wind gusts.

It should also be noted that any nonrotating body is aerodynamically unstable without fins or guidance surfaces. Vertical fins stabilize the yaw, and horizontal fins stabilize the pitch. The pitching movement developed by the fins decreases the angle of attack. This moment opposes the tendency for the nose to rise. It is necessary for the vehicle to remain pressurized and retain a constant shape. The drag coefficient and the lift coefficient are directly proportional to the angle of attack and, therefore, the angle of attack is generally reduced, to minimize cable tension.

Since the Aerocap is generally inflated without the protection of a hangar, inflatable fins are used. A rigid fin is more susceptible to permanent damage. An inflatable fin will recover its original shape even after it has been deformed. Furthermore, the inflatable fin is generally lighter for a given projected area.

A.4 CONSTRUCTION

The balloon designed for the experiment under consideration during Operation Hardtack was designated as a 23-3-5 Aerocap. The physical parameters are shown in Table A.1. The construction methods were those conventionally used by General Mills, Inc. Figure A.1 shows the actual Aerocap inflated ready for raising. The several units which make up the balloon are described below.

A.4.1 Shroud. The shroud was constructed of high-tenacity nylon sewn together with orlon thread. The nylon weighed 2.7 oz/yd^2. Nylon webbing was sewn into the shroud as a reinforcement where stress concentrations occurred. The main purpose of the shroud was to carry the load.

A.4.2 Liner. The gas-retaining liner was fabricated from 2½-mil polyethylene and contained an air reservoir called a ballonet. The ballonet had a capacity of 400 cubic feet. It decreased in volume as the helium expanded during ascent and vice versa during descent, thus maintaining a constant shape for the balloon. The ballonet was pressurized by a battery-operated centrifugal blower.

A.4.3 Harness. The balloon was restrained by twenty aircraft cables. Each cable was terminated

by a clevis and D ring at the balloon. The D rings were attached to the shroud with three lengths of nylon webbing in a crowfoot pattern. The lower ends of the harness cables were attached to an I-beam. Eight of the twenty cables were $\frac{3}{32}$-inch aircraft cables and the remainder were $\frac{1}{16}$-inch aircraft cables.

TABLE A.1 PERTINENT AEROCAP DATA

Volume	18,400 cubic feet
Diameter	23 feet
Length	69 feet
Aerocap and accessory weight	434 pounds
Tethering cable weight	300 pounds
Pay-load weight	250 pounds
Static free lift	170 pounds
Battery life	24 hours
Design and maximum flying altitude	2,000 feet MSL

A.4.4 Fins. The stabilizing fins were air-inflated structures fabricated of nylon and polyethylene in much the same manner as the envelope. The fins were constructed with ribs which caused the cross section to appear as several connected cylinders.

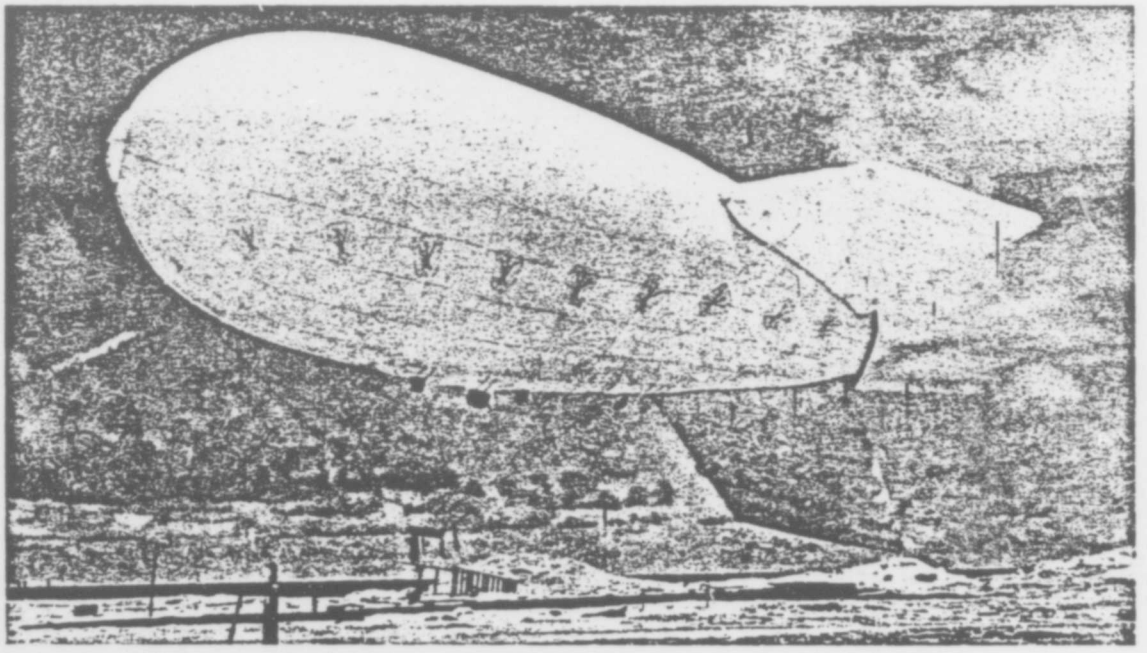

Figure A.1 Aerocap balloon, Model 23-3-5.

A.4.5 Accessories. Incorporated into the Aerocap were safety devices such as a flashing red light to mark the balloon at night, and colored pennants to mark the cable during the day. The mooring cable had a weak link where it connected to the balloon. The link consisted of a short length of $\frac{3}{16}$-inch aircraft cable, whereas the rest of the cable was $\frac{7}{32}$-inch aircraft cable. This safety device would prevent any loss of instrumentation should the balloon break away.

The electric power for the air blowers was furnished by one 24-volt (3151 Rebat) aircraft battery and one 12-volt (R-19 Rebat) aircraft battery. The ballonet was pressurized by two blowers operating at 12 volts, whereas the fins were pressurized by one blower operating at 24 volts.

The nose valve had a spring-loaded door approximately 8 inches in diameter which could be opened to deflate the balloon. The nylon line securing the valve was severed by two General Mills explosive cutters when actuated by an electric current.

A relief valve was provided in the ballonet to release the ballonet pressure during ascent. The relief valve was necessary since check valves were used on the

blowers. The air passed into the ballonet through the blowers and out through the relief valve. The check valves were safety devices that permitted passage of air in one direction only.

A.5 OPERATIONS

A.5.1 Mooring System. The mooring system as originally planned was a four-wire pentahedron with a single wire between the apex and the balloon as shown in Figure A.2. The height of the apex was 400 feet. The instrumentation positioned below the 400-foot level was attached to a cable suspended from the apex and connected to a block 108 feet from ground zero at an azimuth of 189 degrees. The apex was positioned over a point 100 feet from ground zero at an azimuth of 273 degrees.

The pentahedron was formed by four lengths of $^{7}/_{32}$-inch aircraft cable. The length of each cable was controlled by one of two double-drum winches as shown in Figure A.3. Sheaves were attached to concrete blocks to form the basis of the pentahedron. Two blocks were buried in the coral, and two were located in the water. The block located on the ocean-side reef was never under water, but the lagoon-side sheave was attached to a buoy that was continuously submerged. The tide had little effect on the position of the sheave.

The apex of the pentahedron maintained a relatively fixed position, because the cables were in constant tension. The tension in each leg varied as the wind direction changed, but the downwind leg had the least tension and, therefore, the greatest catenary. The apex moved whenever a catenary changed. Since the movement of the apex was relatively small, the slant range between the instruments on this line and ground zero was practically fixed. Each instrument station weighed 13 pounds and was connected to the main cable as shown in Figure A.4. The upper end of the instrumentation unit was snapped onto a $1^{1}/_{4}$-inch-diameter

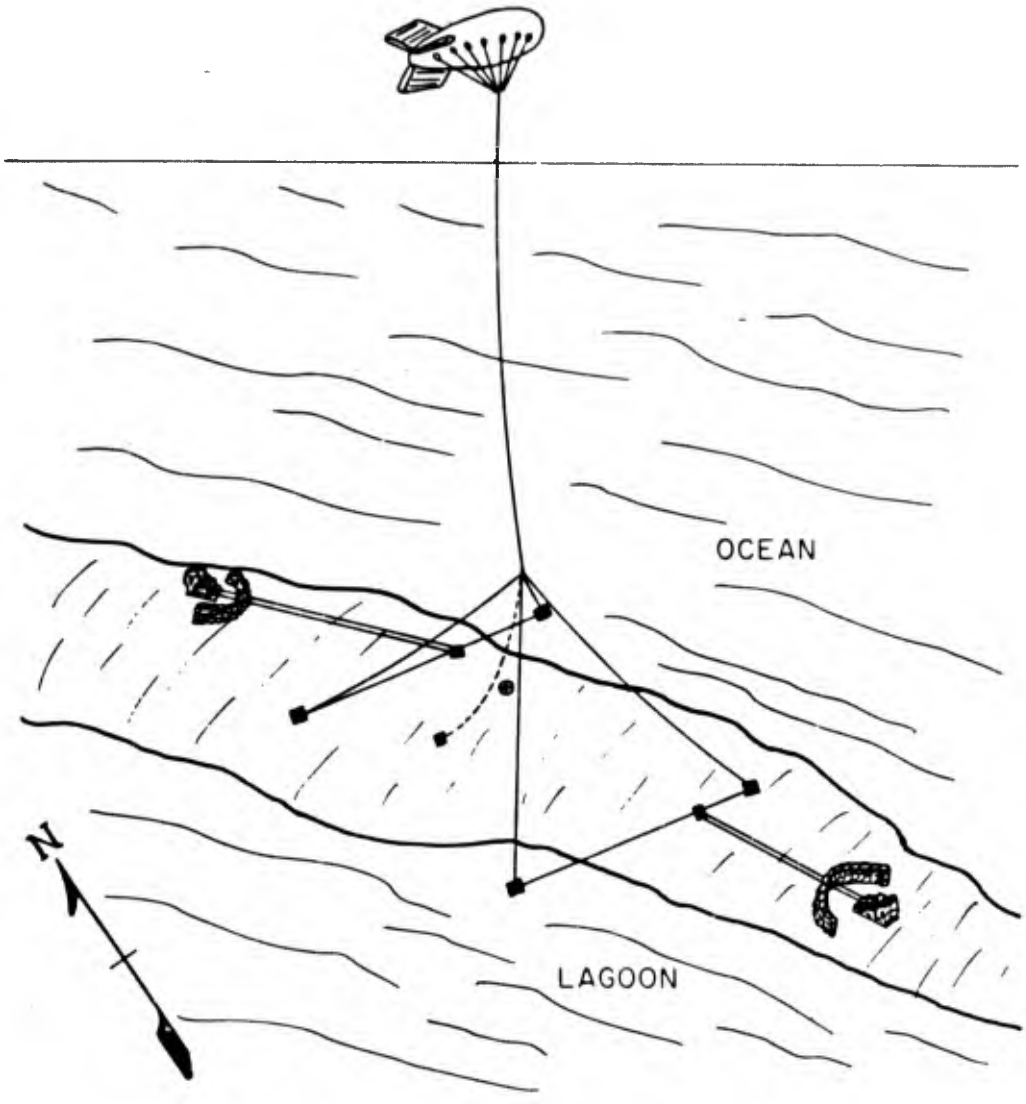

Figure A.2 Balloon-anchoring arrangement, Shot Quince.

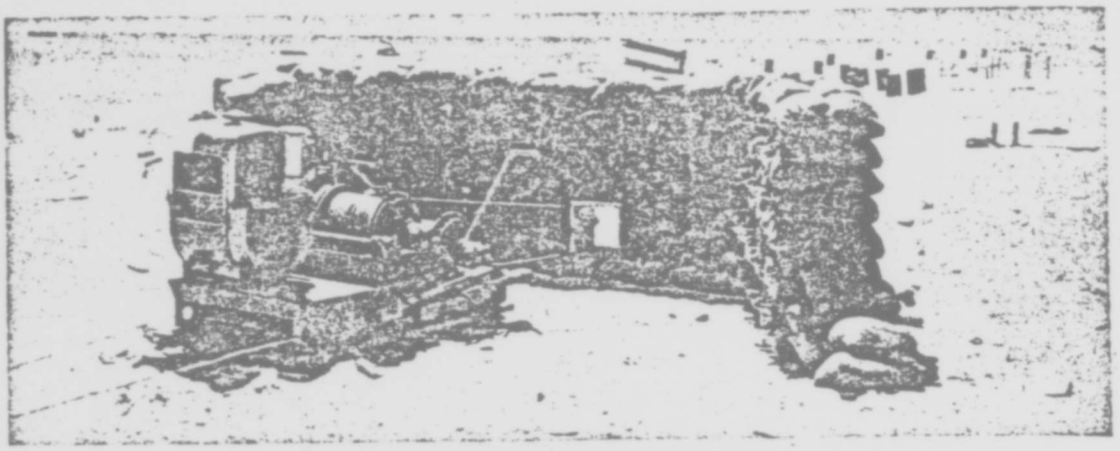

Figure A.3 Winch and blast shield.

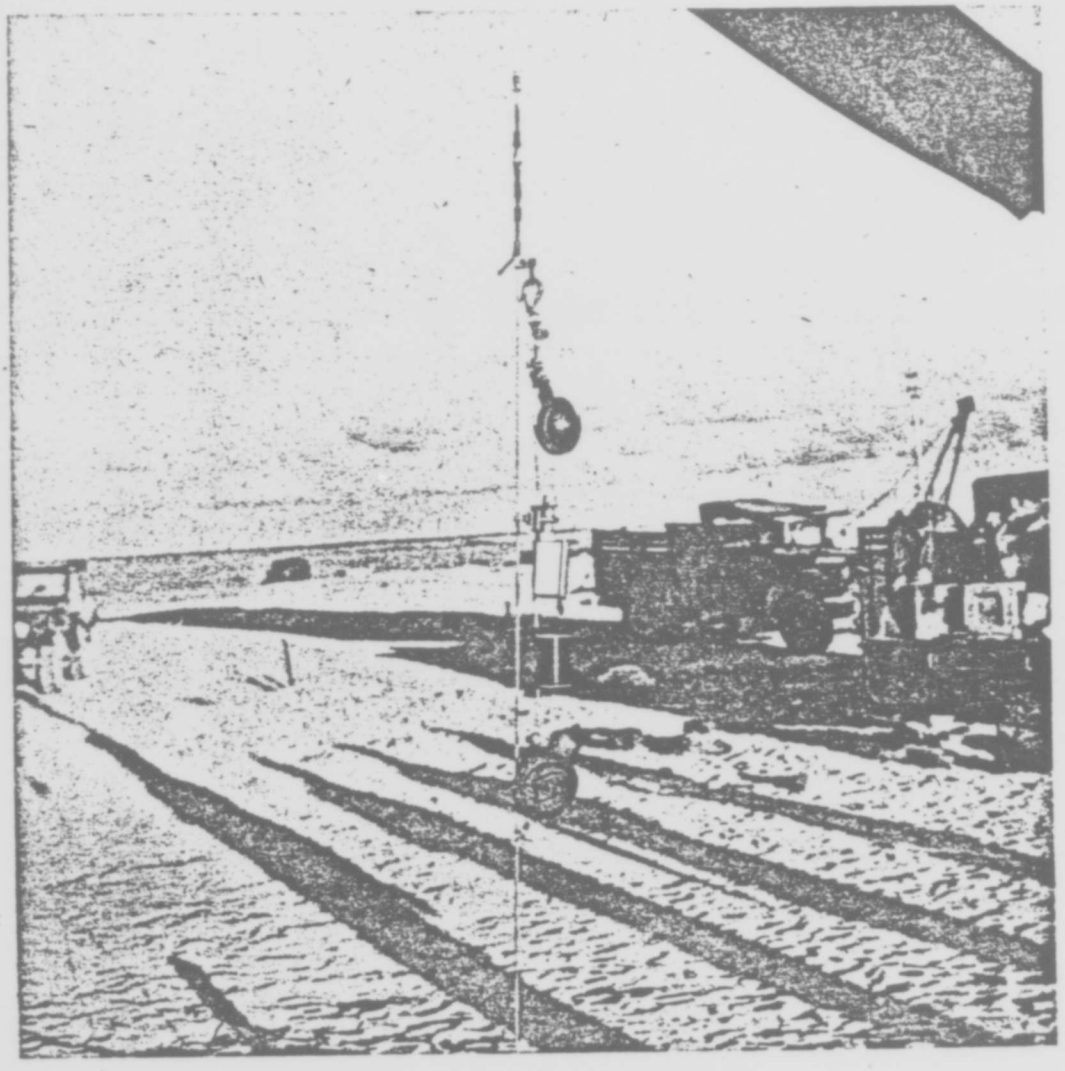

Figure A.4 Instrumentation attachment.

ring and connected to a special fixture which was secured to the cable by tightening a wing nut. The center and lower end of the instrument unit was taped to the cable.

A theodolite was used to determine the downwind position of the balloon after it was raised. The instrument was located at Station 1520 on the shot island prior to shot time and was used to follow the movement of the balloon. The slant range was determined by assuming the cable was a straight line and measuring the deviation from the vertical. The fixes taken from Station 1520 were used to verify the position.

A.5.2 Inflation. The balloon was laid out on a ground cloth which was surrounded by eight concrete blocks with sheaves attached. There were three equidistantly spaced blocks on each side and one near both the nose and tail. Nylon line was secured to ten of the D rings of the balloon harness reinforcements and passed through the sheaves to a winch. The nylon lines held the balloon close to the ground during the initial part of the inflation as shown in Figure A.5. As the balloon assumed its correct shape, the nylon lines were released, and the load was transferred to its regular harness.

Before the envelope was inflated with helium, the fins and ballonet were inflated with air by means of the auxiliary blowers. The fins were checked for leaks and for possible nonalignments. Although the fins exposed large surfaces to the wind, they were easier to handle when pressurized.

The helium for the first two inflations was stored in helium trailers. The other supply was stored in small cylinders and required special manifolding in order to speed up the inflation. One hundred and fifteen cylinders were used for each inflation. The helium was transferred into the balloon through an inflation tube attached to the tail fitting of the balloon. The tube was rolled up and placed inside of the fitting after inflation was completed.

A.5.3 Raising. The balloon was inflated near the sheave on the south leg of the pentahedron. It was raised 1,100 feet over this point before the collector ring was bolted to the main cable as shown in Figure A.6. This collector ring supported the instrument line and the other three legs of the pentahedron. The main cable was raised approximately 300 feet more before the other cables were tightened. The balloon was then moved into position by adjusting the lengths of each leg of the pentahedron.

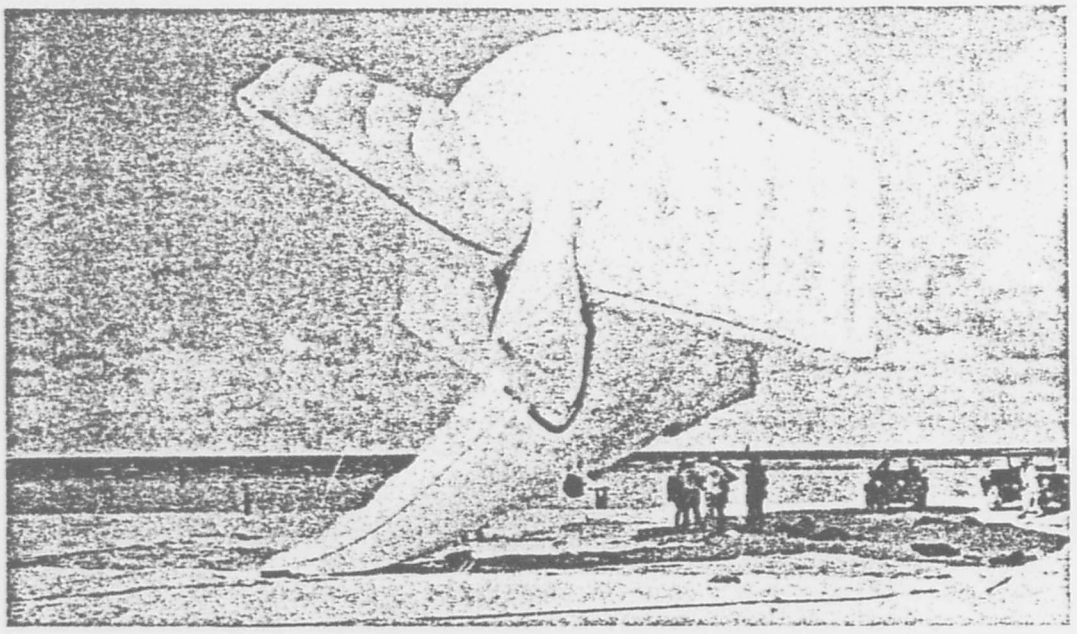

Figure A.5 Balloon inflation.

A.6 RESULTS

The balloon achieved the objectives set forth in the operational plan for the flight tests. The lateral excursion of the pentahedron apex was less than 8 feet in a steady 12-knot wind for a period of 1 hour. The balloon flew 6 degrees downwind from the vertical. Position stability of the pentahedron apex was influenced by the variation in both wind direction and wind velocity. The former was the most important factor.

The following is a history of each Aerocap flight made before and during Operation Hardtack.

A.6.1 Test Flight. The test flight of Aerocap Number 1 was conducted at Fort Ripley, Minnesota, 12

July 1958. Layout began at 0545 hours. After inflation, the balloon produced a gross lift of 1,155 pounds. The balloon weighed 435 pounds, and the tethering cable weighed 250 pounds. A 300-pound ballast container was added at the apex of the pentahedron to simulate the pay load. The angle of attack was 11 degrees. The flight was successful.

A.6.2 Dry Run at EPG. The dry run began at 0810 hours, 27 July 1958, on Site Yvonne. Aerocap Number 1 was inflated by 1000 hours. The harness was readjusted to reduce the angle of attack to 8.5 degrees. The balloon attained its position at 1,100 feet on a single cable by 1500 hours.

The balloon was lowered at 1610 hours and deflated. It was covered with the ground cloth and sand-bagged for the night. The liner was removed on the following day.

The liner was replaced on 8 August. Wind conditions during that day were favorable. The winds were steady in direction and 6 to 8 knots in velocity during the first part of the day. At 1500 hours the winds at 1,500 feet MSL were 12 to 18 knots. The balloon rode out a rain squall, and deflation was delayed for 1 hour to permit drying.

A.6.3 Shot Quince. Aerocap Number 2 was inflated at 1500 hours, 4 August 1958, at the test site. The gross buoyancy was 1,165 pounds. The tail pressure was 2.25 inches of water. The Aerocap was ready for raising at 1825 hours. Eleven hundred feet of cable were dispensed and five samples were attached in their respective positions in 13 minutes. The balloon was not positioned that night because of darkness.

At 0800 hours, on 5 August, the balloon was moved into position and a theodolite fix was taken on two parts of the instrumentation. Later in the day, the test was postponed, and the balloon was lowered to change the batteries and check the free lift. It had lost 300 pounds of lift. After being refilled with 45 bottles of helium, the balloon was raised to 1,100 feet for the night.

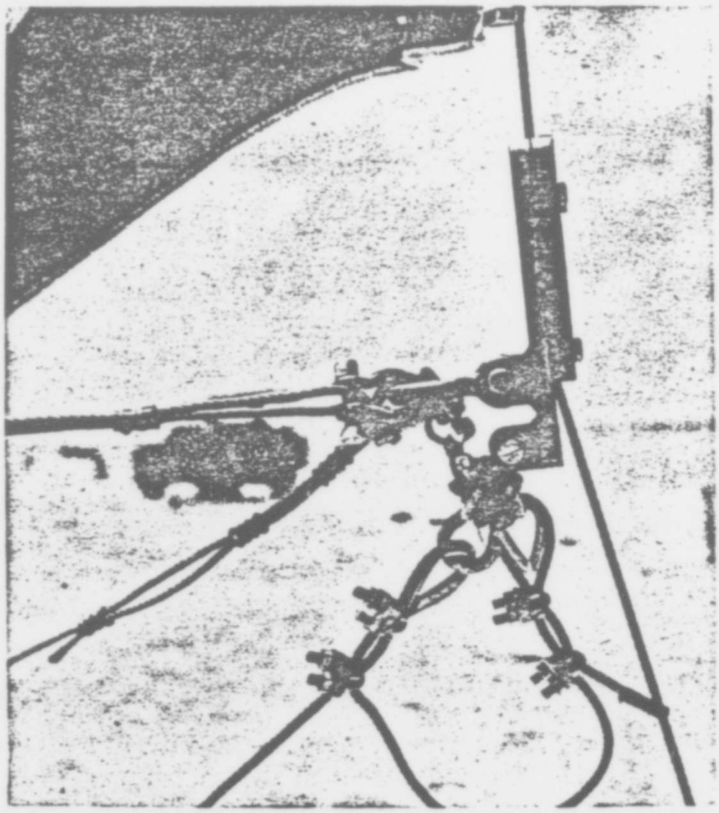

Figure A.6 Pentahedron-apex collector ring.

When the crew returned to the island at 0630, on 6 August 1958, the balloon had lost lift to the extent that it was no longer pressurized. Because of the shortage of time before the shot and the danger to other projects in the area, the balloon was destroyed.

Permission was granted to inflate another balloon if the job could be accomplished and the area cleared by 1300 hours. With the help and cooperation of many people in the Task Group, Aerocap Number 3 was inflated and in position by 1300 hours. It was necessary to manifold 115 small cylinders of helium and subsequently measure the lift with a dynamometer. The surface winds were 15 to 20 knots during the entire inflation. The angle of attack was 3 to 4 degrees, and the balloon crabbed into the wind at 15 degrees. Be-

cause of lack of time, the flight crew was unable to retrim the balloon. Nevertheless, the balloon's performance did not affect the apex of the pentahedron. The anchoring arrangement is shown in Figure A.2.

The test was completed according to schedule, and the instrumentation was recovered in 20 minutes. After recovery, the balloon was tethered on a single cable approximately 10 feet long. The area was then vacated because of radiological contamination.

On the following morning, the balloon was missing; the safety link had parted during the night.

A.6.4 Shot Fig. Aerocap Number 1 was inflated at at 0130 hours on shot day at the marine ramp on the island of Yvonne. A new gas liner and tail liners had been installed on the previous day. The balloon was moved to the test site with a caterpillar tractor and was ready for raising at 0500 hours. Before the cable was released, two rain squalls lasting 1 hour passed over the island. The balloon absorbed 150 pounds of water, and the angle of attack increased from 8.5 degrees to 15 degrees. Later the angle of attack was reduced as the water on the tail evaporated. The balloon flew into the wind except when it was at a high angle of attack after the rain squalls.

Because of possible danger to the research device if the rain continued while the balloon was in position, it was decided that the balloon be flown on one cable at 1,200 feet MSL. (On a previous flight, the balloon lost altitude after a rain squall, and the cable going to the ocean side dropped over the tent at ground zero. No damage was done, but a potential hazard was recognized.) The thermal detectors were eliminated, to reduce pay-load weight.

The mooring point was 358 feet from ground zero at an azimuth of 154 degrees. Detectors were attached at 100, 200, 400, 600, 800, 1,000, and 1,200 feet from

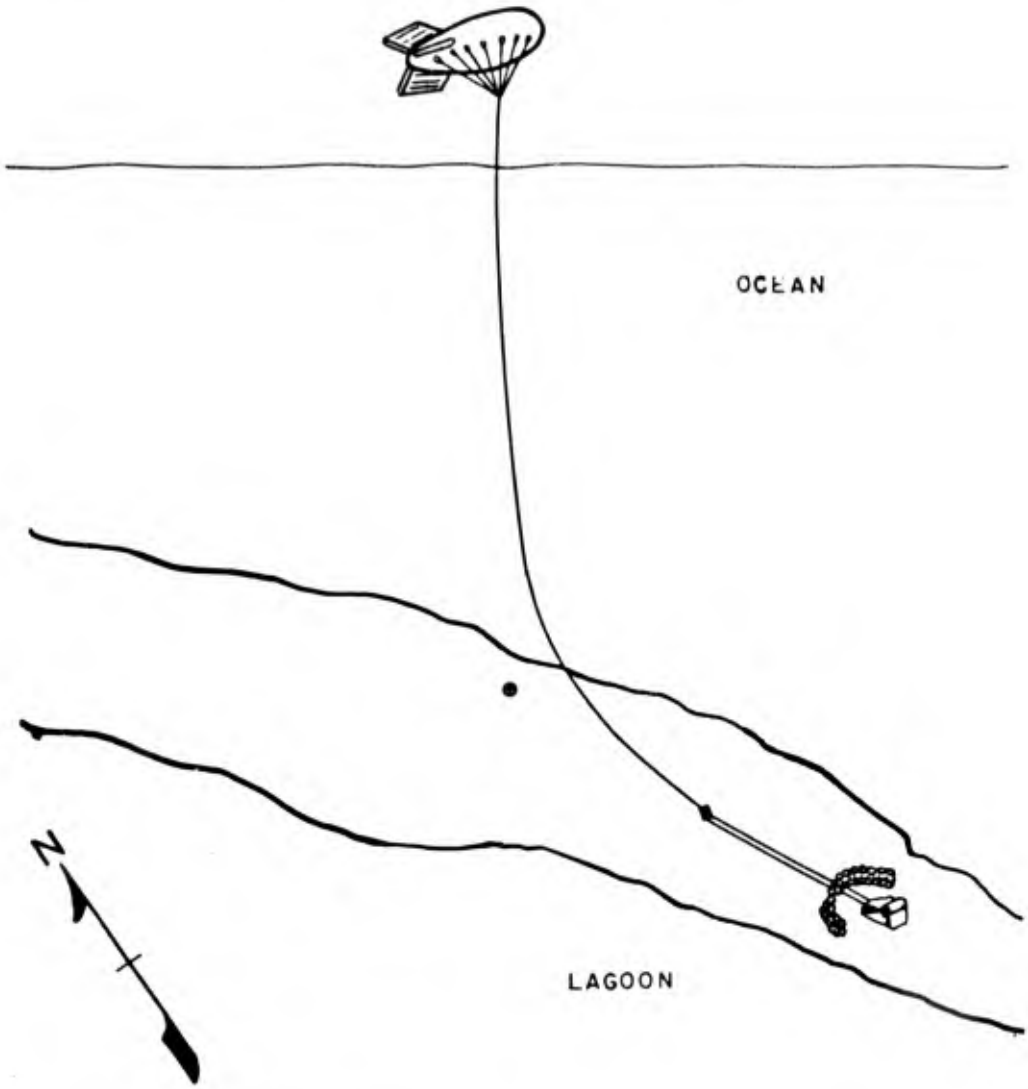

Figure A.7 Balloon-anchoring arrangement, Shot Fig.

the lower end of the cable. The anchoring arrangement is shown in Figure A.7.

The slant range from each detector to ground zero was calculated by assuming that: the wind direction was 90 degrees, the cable was a straight line, and the variation from the vertical was 10 degrees at zero time. The slant range of each detector for Shot Fig is shown in Table 2.4. These assumptions are within the accuracy of the instruments used. The tolerances ± 20 feet for the slant range distances.

A theodolite fix was taken on the balloon harness from the mooring point. The elevation was 80 degrees and the azimuth was 231 degrees. Later the theodolite was positioned beside Station 1520. Observations were made intermittently during the next 8 hours. The elevation angle ranged from 15.9 to 16 degrees, while the azimuth varied between 3.5 and 4.5 degrees. The ground distance from the theodolite to ground zero was approximately 4,750 feet.

During the 8 hours prior to zero time, the wind direction changed from 50 degrees to 90 degrees, the wind velocity varied 13 knots, and the maximum lateral excursion of the balloon was 50 feet or 4 percent of the altitude. The winds at 1,000 feet averaged 17 knots blowing from 90 degrees at zero time.

The nuclear device was detonated at 1600 hours. Recovery was conducted as scheduled except for the time lost in finding gasoline to refuel the winch. The recovery was 50 percent completed when the winch stopped. Extra gasoline was located in the area, and the recovery continued. All personnel were out of the radex area by 1622 hours. The cable holding the seventh detector line was severed during the blast, and the detector was not found.

The balloon was split from end to end at the time of the blast. Since the opening was along the bottom, the material formed a parachute and maintained tension in the cable. After recovery the balloon was moored 2 feet from the ground, and sandbags were placed on the fins.

REFERENCES

1. "Scientific Director's Report"; Operation Sandstone, Volume 8, Annex R, Part K and Addendum, 1948; Secret Restricted Data.

2. W.A. Biggers and others; "Neutron Measurements: External Neutron and Gamma Flux Measurements by Sample Activation"; Annex 1.5, Part II, Section 1, Operation Greenhouse, WT-114, 1951; Los Alamos Scientific Laboratory, Los Alamos, New Mexico; Secret Restricted Data.

3. W.A. Biggers and L.J. Brown; "External Neutron Measurements with Threshold Detectors"; Project 17.1, Operation Upshot-Knothole, WT-826, March 1955; Los Alamos Scientific Laboratory, Los Alamos, New Mexico; Secret Restricted Data.

4. W.A. Biggers, L.J. Brown and K.C. Kohr; "External Neutron Measurements"; Project 14.1, Operation Castle, WT-952, October 1955; Los Alamos Scientific Laboratory, Los Alamos, New Mexico; Secret Restricted Data.

5. C.W. Luke and others; "Neutron-Flux Measurements"; Project 2.51, Operation Redwing, WT-1313, September 1959; U.S. Army Chemical Warfare Laboratories, Army Chemical Center, Maryland; Secret Restricted Data.

6. D.L. Rigotti and others; "Neutron Flux from Selected Nuclear Devices"; Project 2.3, Operation Plumbbob, WT-1412, April 1960; U.S. Army Chemical Warfare Laboratories, Army Chemical Center, Maryland; Secret Restricted Data.

7. J.W. Kinch and others; "Neutron Flux from Large-Yield Bursts"; Project 2.4, Operation Hardtack, WT-1622, May 1960; U.S. Army Chemical Warfare Laboratories, Army Chemical Center, Maryland; Secret Restricted Data.

8. E.N. York, R.E. Boyd and J.A. Blaylock; "Initial Neutron and Gamma Air-Earth Interface Measurements"; Project 2.10, Operation Plumbbob, WT-1419, February 1960; Air Force Special Weapons Center, Kirtland Air Force Base, Albuquerque, New Mexico; Confidential Restricted Data.

9. G.S. Hurst and others; "Technique of Measuring Neutron Spectrum with Threshold Detector—Tissue Dose Determinations"; The Review of Scientific Instruments, Volume 27, No. 3, March 1956; Unclassified.

10. G.S. Hurst, R.H. Ritchie, and H.N. Wilson; Scientific Instrument 22, 981; 1951; Unclassified.

11. E.J. Hart and others; "Radiation Research"; 4, 146; 1954; Unclassified.

12. M.E.J. Carr; "Nature"; 167, 363-4; 1954; Unclassified.

13. G. Weiss and others; "United Nations Conference for the Peaceful Uses of Atomic Energy"; 179-181; 1955; Unclassified.

14. W.H. Moncrief, Jr. and others; "Effects of Very-Low-Yield Bursts on Biological Specimens (Swine and Mice)"; Project 4.2, Operation Hardtack, ITR-1663, June 1959; Walter Reed Army Institute of Research, Walter Reed Army Medical Center, Washington 12, D.C.; Secret Restricted Data.

15. M. Morgenthau and J.C. Maloney; "Gamma-Dose Measurements from a Very-Low-Yield

Burst"; Project 2.9, Operation Hardtack, ITR–1677, March 1959; U.S. Army Chemical Warfare Laboratories, Army Chemical Center, Maryland; Confidential Formerly Restricted Data.

16. J.J. Mahoney and others; "Thermal Radiation from Very-Low-Yield Bursts"; Project 8.7/2.12d, Operation Hardtack, WT–1676, June 1960; U.S. Army Chemical Warfare Laboratories, Army Chemical Center, Maryland, and U.S. Naval Radiological Defense Laboratory, San Francisco 24, California; Confidential Formerly Restricted Data.

17. J.W. Kinch and D.L. Riggoti; "An Activation Type Neutron Detection System and Its Calibration"; CWLR 2282; U.S. Army Chemical Warfare Laboratories, Army Chemical Center, Maryland; Confidential Formerly Restricted Data.